Structure, Morphological, and Physicochemical Characteristics of a New Composite Coagulant Made From Polyaluminium Chloride and Agro-waste of Tapioca Peel

Mohd-Salleh SNA
  Universiti Tun Hussein Onn Malaysia   https://orcid.org/0000-0002-2902-6031

Shaylinda MZN (✉ nursha@uthm.edu.my)
  Universiti Tun Hussein Onn Malaysia

Othman N
  Universiti Tun Hussein Onn Malaysia

Yashni G
  Universiti Tun Hussein Onn Malaysia

Norshila AB
  Universiti Tun Hussein Onn Malaysia

Sainudin MS
  Universiti Tun Hussein Onn Malaysia

Abstract

A combination of a metal coagulant with an organic polymer can complement both the outstanding and flaw properties of the separate elements. A novel composite coagulant of polyaluminium chloride (PAC)-tapioca peel extract powder (TPP) called PACTPP with different weights ratio was prepared in this study. In the preliminary study, PACTPPg at the weight/weight ratio of TPP/Al=3.71 was selected as the optimum one based on the performance in treating wastewater sample of landfill leachate. Through all characterisation analyses, it revealed that the novel composite reagent exhibits better coagulant properties when compared with the individual coagulants of PAC and TPP. It was characterised that PACTPPg had combined the best benefits from PAC and TPP, with an acidic property of pH 3.45, the low charge density of 3.45 mV, the higher molecular weight of 1.59×10^7 g/mol, the bigger particle size of 4.528×10^4 d.mn, and a longer connected and compact structure. Through Fourier transform infrared (FTIR) and X-ray diffraction (XRD) analyses, PACTPPg was identified to comprise new chemical compounds, i.e., the functional groups of ketones, aldehydes, and alkanes in a semi-formed crystalline phase. Based on the comparison study, it can be concluded that PACTPPg showed a correlation to encompass the complex interpenetration networks rather than just a simple mechanical mixing of raw materials.

1. Introduction

1.1 Development of composite coagulant

The application of synthetic polyelectrolytes as primary coagulants (cationic polyelectrolytes) and coagulant aids (anionic and non-ionic polyelectrolytes) often used as a dual coagulant are the conventional step for further binding the small flocs into bigger agglomeration. By doing so, faster and stronger formation of flocs, lower coagulant dosage volume, and higher reduction of impurities are hopefully achieved [1]. It is undeniable that a dual coagulant can reduce the dose of the chemicals used, thus minimising the toxicological effect. However, it is considered time-consuming as the process involves two distinct steps. Due to these limitations, the innovation to initiate the composite or hybrid coagulants is emerging. As stated by Shaylinda *et al.* [2], a composite coagulant is made by combining two types of coagulants as one reagent by premixing the coagulants through certain working conditions. The substitution of chemical coagulants with natural materials can be applied to reduce the adverse effects, simplify the dosing process, and tackle other drawbacks [2, 4]. The operation using a composite coagulant is more convenient as it shortens the treatment process and practical from a financial perspective.

The growing demand for efficient and sustainable materials in the industry of wastewater treatment has become the next emerging factor for the development of composite coagulants from many potential constituents, e.g., organic and natural polymers [5]. The addition of alternative additives into the composition of pre-polymerised coagulants as a single mixture is considered a reasonable effort due to its broader applications [6]. Consequently, the utilisation of both terms of 'composite' and 'hybrid' by researchers to describe a newly modified reagent technically has the same definition regardless of their properties. As stated by Lee *et al.* [5] and Nanko [7], there are three prime groups to classify the preparation of composite coagulants, i.e., structurally-hybridised materials (composites), chemically-bound-hybridised materials, and functionally-hybridised materials.

1.1.2 Potential of composite coagulant as a future alternative

Composite coagulants have good potential to be commercialised as sole coagulants that can improve coagulation performance and overcome the time-consuming process. The association of both materials has been reviewed by past studies, where many studies have interests in synthesising inorganic-inorganic [6, 8] and inorganic-organic materials [5]. A study by Moussas & Zouboulis [8] stated that the new combination of materials increased the polymer species concentration and promoted excellent properties of coagulants. Increasing the number of polymeric species in the original structure or producing new composite coagulants to be used with other components are the techniques that can improve the coagulation-flocculation efficiency [8]. They also exhibit good stability, which is better than a single primary coagulant [9] as the increased molecular size enhances the aggregation ability. It is assumed that high molecular weight coagulants are more effective in improving the bridge formation capability among colloidal particles [10] due to the intrinsic unity of relation among the floc properties under various coagulation mechanisms. The newly developed composite coagulants also imposed functional groups that are useful as coagulating agents as studied by Yang *et al.*

[11], Wang *et al.* [12], Chen *et al.* [13], Li *et al.* [14], Chen *et al.* [15], and Huang *et al.* [9]. Table 1 highlights the characteristics of new composite coagulants of the identified functional groups through FTIR analysis from previous studies.

Table 1 Functional groups identified in several composite coagulants

Composite Coagulant	Absorption Range/ Wavelength Peak (cm^{-1})	Identified Functional Groups
Polymeric ferric aluminium sulphate chloride (PFASC) [11]	3334–3369 cm^{-1}	Stretching vibration of $-OH$ groups
	1630–1631 cm^{-1} 1400–1402 cm^{-1}	Bending vibrations of $-OH$ groups in water molecules
	1026 cm^{-1}	Asymmetric stretching vibration of Fe-O-Fe or Al-O-Al
	806 cm^{-1}	Bending vibration of Fe-OH-Fe or Al-OH-Al
	625 cm^{-1}	Bending vibration of Fe-OH and Al-OH
	515 cm^{-1}, 478 cm^{-1}	Winding vibration of Fe-O and Al-O
Polyferric chloride polydimethyl-diallyl-ammonium chloride (PFC-PDM) [12]	3600–3200 cm^{-1}	Stretching vibration of $-OH$ (H-O-H angle distortion frequency)
	1700–1600 cm^{-1}	Bending vibration of $-OH$ groups (H-O-H angle distortion frequency)
	3600–3000 cm^{-1}	Stretching vibration of $-OH$
	865 cm^{-1}	Possibly the bending of Fe-O-Fe or Fe-OH-Fe
	670 cm^{-1}	Bending vibration of Fe-O-H
Polymeric ferric titanium sulphate (PFTS) [13]	3250–3500 cm^{-1} Peak at 3437 cm^{-1}	Intermolecular association stretching vibration of $-OH$
	1600–1650 cm^{-1}	Bending vibration of the water absorbed, polymerised, and crystallised in the coagulant
	Peaks at 1134 and 1127 cm^{-1}	SO_4^{2-} symmetrical and anti-symmetrical stretching vibration
	998–1068 cm^{-1}	Asymmetric stretching vibration of Fe-OH-Fe or Ti-OH-Ti
	470–664 cm^{-1}	Stretching vibration of Fe-O bonds and bending vibration of Fe-OH and Ti-OH
	Peak at 538 cm^{-1}	Stretching vibration of Ti-O bond
Poly-ferric-magnesium polydimethyl-diallyl-ammonium chloride (PFM-PDMDAAC) [14]	1398 cm^{-1}	attributed to the $-CH_2^-$ adsorption
	1075 cm^{-1} and 998 cm^{-1}	Hardly observable in the PFM spectrum and absent from the PDMDAAC spectrum and it is suggested that some new chemical compound had formed
Polyferric aluminium silicate sulphate [15]	1637–1633 cm^{-1}	Stretching vibration of $-OH$
	Peaks at 1400 cm^{-1} and 2450 cm^{-1}	Al-O-Al bonds stretching and bending vibration
	Peaks around 500 cm^{-1}	Stretching vibration of Al$-$O bonds
	1099–1137 cm^{-1}	Asymmetric stretching vibration of Fe-OH-Fe or Al-OH-Al
	977–999 cm^{-1}	Bending vibration of Si-O-Al or Si-O-Fe bonds

	596–611 cm^{-1}	Fe-O groups
Polytitanium silicate sulphate (PTSS) [9]	Strong and broad peaks at 3500–3300 cm^{-1} and 1642 cm^{-1}	Attributed to the stretching vibration of −OH and to the vibration of water absorbed, respectively
	1367 cm^{-1}, 1112 cm^{-1}	Si-O-Si bonds
	1007 cm^{-1}, 1030 cm^{-1}	Si-O-Ti bonds
	400–700 cm^{-1}	Stretching of Ti-O bonds

The flocculating performance of coagulants also gets influenced by the specific chemical bonding properties of the polymer, especially those that comprising various functional groups. The particular groups to be estimated are OH$^-$ and COO$^-$ as their existence usually contributes to the flocculating activity of coagulant. Besides, the increase in positively charged functional groups allows more interactions with the negatively charged colloidal particles, thus improve the binding capabilities between them [16]. Previously, Zhou et al. [17] had formulated a novel inorganic-natural polymer composite of polyaluminium ferric chloride-starch graft copolymer with acrylamide and dimethyl diallyl ammonium chloride (PAFC-Starch-g-p(AM-DMDAAC)) for textile wastewater treatment. The new coagulant managed to reduce about 50% of the dosage. It demonstrated better storage ability, which depicted its favourable prospects in lowering the operational cost and only a single unit of dosing method is required. Additionally, the process of physical blending might not generate new chemical bonds as experienced by Wang et al. [12], who studied the composites of polyferric chloride (PFC) and polydimethyldiallylammonium chloride (PDM) (PFC-PDM). However, it is acknowledged that the primary goal of preparing a composite coagulant is to combine all the benefits of synthetic or natural coagulants while tackling their limitations [18]. Nevertheless, researchers who have developed composite coagulants preferred to use the combination of inorganic-inorganic coagulants with little attention to developing coagulants from agro-waste.

1.2 Chemical coagulant of polyaluminium chloride (PAC)

The utilisation of PAC is chosen to complement the development of the composite coagulant in this study due to its benefits, which can cater to the diverse requirements of water treatment plants. PAC also has a good structure of higher charge density and low dosage requirement for excellent coagulant activity in the previously reported studies [15, 20, 21, 22, 23]. According to the study made by Ghafari et al. [20], the optimum pH for PAC was favourably higher than alum and PAC showed efficient results in the physical-chemical treatment when tested on stabilised leachate, which was also highly polluted wastewater. This preformed polymeric metal coagulant produced lesser sludge than alum and has a significant advantage of lower alkalinity [19, 20]. The alkalinity here refers to the capability of water or any solution to neutralise the acid.

The utilisation of PAC is increasingly popular, especially in developed countries like Japan and North America where the material is widely available. Also, the introduction of PAC in water and wastewater treatment has drawn the attention of researchers, thus increasing its demand in the remediation industry due to lower consumption of basicity and superior to other coagulants [19]. However, the price of PAC is quite high in the commercial market [1, 24] due to the complicated preparation procedures even though the raw materials are cost-efficient. The strength of generated flocs after the coagulation-flocculation process is also weak, making the flocs easy to scatter and disperse again [25, 26]. On the other hand, the high cost of raw materials is a real concern to be dealt with. The producing cost of this pre-polymerised aluminium salt has been declared crucial to develop more capable coagulants for the future's sake. Therefore, as a remedy to this situation, the utilisation of natural materials is introduced [27].

The search for eco-friendly and sustainable treatment processes is always encouraged as the effort gives many benefits to others. Natural coagulants extracted from plants contain polysaccharides and proteins. The polysaccharides originate from carbohydrates, with glycosidic bonds linked to its sugar rings. Therefore, polysaccharides would behave like polyelectrolytes when charges are available [28]. The present coagulating characteristics make them safe for consumption in wastewater treatment. As stated by Theodoro et al. [29], the reduction or replacement of these coagulating agents adds value to the sources of origin, while avoiding the chemical and physical post-effects in the treated medium. These issues, together with the increase in awareness of sustainable development, have driven the water treatment sector to search for natural coagulants.

1.3 Brief overview of Manihot esculenta plant

Cassava or *Manihot esculenta* is a perennial woody shrub, which is a member of the Euphorbiaceae family that is typically grown as an annual crop in the tropical climate of the Amazon basin, Latin America, African region, and Asian countries [30, 31]. The cultivation of cassava is well-recognised as tapioca especially among Asians, with a large tuberous root that becomes the common low-cost carbohydrate food source for populations in the developing regions [31, 32]. According to Zhang *et al.* [30], based on the production data of 2000−2014, Asia is one of the leading regions alongside America and Africa in the cultivation of tapioca, which is cultivated by small-scale farmers. The secure custody and numerous benefits of tapioca towards producers have become the ultimate reasons for this choice of the crop in the sustainable agricultural sector. The cultivation of tapioca is claimed to be trouble-free due to its ability to grow well even with insufficient nutrients and the wide range pH (4.0−8.0) of infertile soil [33, 34]. It is a tropical root crop that does not withstand freezing conditions and requires a minimum of eight months of warm weather before harvesting [33]. Generally, the composition of the tapioca root includes the central vascular fibre, starchy flesh, cortex, and periderm,

Tapioca peel originally comes from cassava/tapioca root (*Manihot esculenta*), i.e., abundantly cultivated in Malaysia. It is considered as the part of tapioca root that does not have any further commercialisation application, besides the use in ethanol, animal feedstock, and activated carbon production. The thickness of the peel can vary from 1 to 4 mm, which is mostly influenced by the nutrients taken by the crop [31]. As stated by Ratnadewi *et al.* [35], tapioca waste is approximately 16% of the total root mass. Meanwhile, the fraction of the waste itself consists of 30% dry weight and 70% water. The dry weight percentage can be further fractioned into 27% hemicellulose, 14% cellulose, 11% lignin, 10% crude fibre, and 3.5% protein, with a little amount of hydrogen cyanide (HCN) content [35, 36, 37, 38]. The harmful content of HCN in peel waste is such a great concern to the environment. As stated by Jain *et al.* [39], agro-waste is a municipal solid organic wastes that could hold a very high moisture content, which is nuisance to the surrounding. The release of HCN to the surrounding is mainly caused by the linamarase enzyme that undergoes cyanogenesis activity on the undisturbed tapioca waste [40]. The water immersion method for several hours is among the few techniques to diminish the harmful content in the waste [35]. Cyanide toxicant could be risky and harmful to living organisms, particularly by interrupting the respiratory system [33]. Thus, the brown peels would be expelled, and only the white flesh of the peels would be taken for further research in this study. Furthermore, tapioca peels have a lower amount of cellulose and holocellulose but rich in hemicellulose [41]. The potential of the peel should be further explored in order to use its benefits to its finest. In this study, the tapioca peel powder (TPP) is recycled and proposed to be a natural coagulant, which can be used in the coagulation and flocculation of water and wastewater treatment.

1.3.1 Potential of tapioca peel powder (TPP) as a natural-based coagulant

Starch has been recognised as the most extensively studied coagulant aid due to its biodegradability and susceptibility to modification [42]. Various past reviews and studies have reported the potential of tapioca peel in water and wastewater remediation [36, 40, 43, 44, 45, 46]. The application of tapioca peel is mostly made in the form of activated carbon, which is also known as a cheap bio-adsorbent in the engineering discipline. The conversion of this agro-waste into activated carbon is acknowledged to extend its lifespan. The peel is chemically modified using the respective concentration of acids to stimulate the particular cell wall and surface [43]. The bio-adsorbent has been widely used for sequestering heavy metal ions [32, 36, 40], mine water treatment [43], gas purification, and fluid detoxification [45]. Agro-wastes such as banana peel, coconut coir, and tapioca peel are proven to have these unique metal-binding sites, which can provide enough capacities to remove heavy metals from polluted water at minimal cost [47]. Besides, the porous surface and the presence of many functional groups (e.g., Si, Mg, Fe, and others) become the key factors to suggest the ability of tapioca peel in removing contaminants.

In addition to the application of inexpensive bio-adsorbent, tapioca peel has also been used as the alternative feedstock for electrode materials used in supercapacitors [40] a packed-bed column using immobilised peel waste biomass, an unmodified organic filter medium [43], cationic waxy tapioca for turbidity and colour removal [29], and a natural coagulant in coagulation-flocculation treatment [44]. The conversion of these by-products into valuable materials would increase their market value and ultimately benefit the producers. It is acknowledged that natural materials, particularly those derived from plants, are often utilised as coagulant aids aside from primary coagulants, e.g., *M. oleifera* seeds, chitosan, and tapioca starch. Nonetheless, relatively little research and further studies have been reported in the literature on recycled agro-waste as natural coagulants. The abundant tapioca peel waste from the small crisp industries, especially around Parit Raja, Johor, Malaysia, has become the continuous source

of this agro-waste as the primary raw material in coagulant development. Despite the toxic component of cyanogenic glucosides in tapioca peel, the peel also contains a detoxification enzyme known as cyanoalanine synthase, which can maintain the cyanide level at the safe level [44].

Meanwhile, the chemical analysis of tapioca peel has also verified the competence of the peel as a natural coagulant through the existence of polysaccharide form of sugars (i.e., holocellulose and starch) and the functional groups (i.e., carboxyl, hydroxyl, and amino groups) from pectin, cellulose, and amino acids, which may also have the potential as a flocculating agent [44]. These groups can be identified through the functional group analysis using FTIR spectroscopy. Oladoja [27] stated that starch consists of two polymers of anhydroglucose units (i.e., amylose and amylopectin), which have been applied as renewable materials in water and wastewater treatment. However, the starch has poor surface charge density that would result in low coagulation efficiency. Consequently, it makes tapioca starch unsuitable to be applied as the primary coagulant in treatment operations. This limitation needs to be modified first to compete with other established coagulants. According to Oladoja [27], in the effort to reduce the amount of the optimum primary coagulant used in the coagulation-flocculation process, raw tapioca starch was applied as an aid in the alum coagulation of Congo red from the aqua system. The use of tapioca starch as a coagulant aid reduced the optimum alum dose by 50%. The applicability of tapioca peel as a potential natural coagulant also has been explored and reviewed in several studies [43, 44, 47].

Through its characterisation using X-ray fluorescence (XRF) spectrometry, tapioca peel contains some elements that could help in the coagulation process, e.g., aluminium oxide (Al_2O_3) and ferric oxide (Fe_2O_3). Furthermore, the presence of silicon dioxide (SiO_2) and calcium oxide (CaO) may also be a big help in strengthening the floc agglomeration by adding the weight and size to particles in treated samples [44]. Therefore, it is an economically-worthwhile approach to discover the potential of recycled tapioca peel that is sustainable to the environment, current, and future livelihood. Several studies referred to the use of alternative coagulants from recyclable materials due to their cost effectiveness [48].

The novelty and the objective of this research are to study the properties of the new-developed composite coagulant of PACTPP in terms of structure and morphological, and physicochemical by considering the characteristics of the individual coagulants, i.e., PAC and TPP for the comparison purpose. Hence, this study aims to determine the synergistic effect between both of the coagulants in order to produce a sustainable composite coagulant of PACTPP.

2. Materials And Methods

2.1 Extraction of TPP starch

TPP was prepared by referring to the methodology of Asharuddin *et al.* [44]. The peels of tapioca were collected from small-medium processing industries in Parit Raja, Johor, Malaysia. Within the same day, the peels were washed with tap water to clean it and to remove all the presented impurities. The peels were subsequently cut into small pieces, and the most (brownish) outer layers were expelled while only the white flesh from the cortex was scratched. The white flesh was blended using domestic blender together with distilled water in a 1:1 ratio. The blended white flesh was allowed to settle down for 24 hours, and the excess distilled water was rinsed out. The white flesh solution was filtered using a cloth filter, filter tunnel, and conical flask. The sticky blended white flesh was spread onto a tray and sundried until completely dry. The powder was stored in a tight container and kept in room temperature for further use. Next, to prepare the TPP coagulant solution, a range of the amount of TPP in grams of was weighed and diluted into 100 ml of distilled water [49, 50], producing the respective concentrations of TPP solution. The solution was stirred on the hot plate of 70-75 °C to promote the starch gelatinisation. Starch gelatinisation is essential to completely dissolve the starch granules, by breaking down the intermolecular bonds of starch molecules in the presence of water and heat.

2.2 Development of composite coagulant of PACTPP

The most common method to prepare composite coagulant is by physical blending [8]. PACTPP was prepared according to the methodology used by Shaylinda *et al.* [2]. The preparation was started by injecting a range of amounts of TPP into a 200 mL solution of a range of amounts of PAC using a peristaltic pump. The injection was done with magnetic stirring (300-400 rpm) to prevent the formation of insoluble products. The preparation of composite coagulant was influenced by different weight ratios of

TPP and PAC, with flow rates of the peristaltic pump at 2 mL/min, and water bath temperature at 70-75 °C. Physical blending with higher temperatures would provide better chemical stability for the composites [5]. The composite coagulant was allowed to age for 24 hours at room temperature and then stored in a laboratory refrigerator.

The procedure was set up as in Figure 1. The preparation of the new composite coagulant consisted of overall 10 different weight/weight ratio of TPP and Al content of PAC (TPP/Al), named PACTPP (a-j). Nevertheless, in the preliminary stage, the optimum PACTPP was decided to be PACTPPg by determining its treatability abilities for the treatment of leachate samples. The performance of PACTPPg in treating leachate could be viewed in the Appendix (supplementary data). The formulation of PACTPPg with different TPP/Al mass ratio is shown in Table 2.

Table 2 Preparation of PACTPPg by different weight/weight TPP/Al ratio

Composite coagulant	PAC (mg/L)	TPP (mg/L)	Amount of PAC, TPP, Al (mg) in 55,000 mg/L of PACTPP			Ratio of TPP/Al
			PAC	TPP	Al	
PACTPPg	70,000	40,000	7,000	4,000	1,078	3.71

Table 2 represents the concentrations (mg/L) of individual PAC and TPP, as well as the content (mg) of PAC, TPP, and Al in PACTPPg. The measurement of Al was desired because each composite coagulant had a different concentration of PAC in the similar 55,000 mg/L concentration of PACTPP. The complete calculations for each concentration were shown as in Eqs. (1)-(4) below;

Concentration of PAC:

$$\underset{\text{(7 grams in 100 mL)}}{7\%} \quad \begin{aligned} &= (7 \text{ g}/100 \text{ mL}) \times (1000 \text{ mg}/1\text{g}) \times (1000 \text{ mL}/1\text{L}) \\ &= 70{,}000 \text{ mg/L} \end{aligned} \quad (1)$$

Concentration of TPP:

$$\underset{\text{(4 grams in 100 mL)}}{4\%} \quad \begin{aligned} &= (4 \text{ g}/100 \text{ mL}) \times (1000 \text{ mg}/1\text{g}) \times (1000 \text{ mL}/1\text{L}) \\ &= 40{,}000 \text{ mg/L} \end{aligned} \quad (2)$$

Total concentration of PACTPP:

$$\frac{4\% + 7\%}{2 \, (/100 \text{ mL})} \quad \begin{aligned} &= (4 \text{ g}/100 \text{ mL}) \times (1000 \text{ mg}/1\text{g}) \times (1000 \text{ mL}/1\text{L}) \\ &+ (7 \text{ g}/100 \text{ mL}) \times (1000 \text{ mg}/1 \text{ g}) \times (1000 \text{ mL}/1 \text{ L}) \end{aligned} \quad (3)$$

$$= 55{,}000 \, \text{mg/L}$$

Al content in 55,000 mg/L of PACTPPg:

$$PAC = Al_2Cl(OH)_5 = 174.75 \, \text{g/m} \qquad (Al=26.982, O=16, H=1, Cl=35.45)$$

$$1 \, \text{mole } Al_2Cl(OH)_5 = 174.75 \, \text{g/ } 1000 \, \text{mL}$$

$$? \, \text{mole } Al_2Cl(OH)_5 = 10 \, \text{g } /100 \, \text{mL}$$

$$= 0.572 \, \text{mole}$$

(4)

$$10 \, \text{g PAC} = ? \, \text{g Al}$$
$$\text{Mass of Al} = (0.1 \, \text{L x } 0.572 \, \text{mole x } 26.982g)$$
$$= 1.54 \, \text{g Al}$$
$$1 \, \text{g PAC} = 0.154 \, \text{g Al}$$
$$7 \, \text{g PAC} = 1.078 \, \text{g AL}$$
$$= 1078 \, \text{mg Al}$$

2.3 Characterisation of coagulant

Characterisation test is required since the prepared composite coagulant (PACTPPg) is considered distinctive and new. The tests are also important in order to gain information related to the finding of the best weight/weight ratio of TPP/Al = 3.71 during the preliminary stage of study [51]. The characterisation tests were conducted after 24 hours of the ageing process. The characterisation analyses were also carried out for other coagulants; single coagulants (PAC and TPP) and dual coagulants (PAC+TPP) to observe the differences. The morphological characteristics and physical-chemical structures of them were discussed for a comparative purpose. The characterisation methods were explained as below:

2.3.1 pH

The prepared coagulants (PACTPPg, PAC, and TPP) were tested with a pH meter (HQ 11D portable pH meter) to know its pH concentration following the electrometric APHA standard method of 4500-H^+ [52]. The pH characteristic is vital since it can alter the pH of the leachate sample, even at the slightest change. The calibration of the pH meter was carried out before the measurement of pH activity. A mean of three readings was taken for this measurement.

2.3.2 Scanning electron microscopy/energy-dispersive x-ray (SEM-EDX)

SEM-EDX technique was used to determine the high-resolution image of morphology and surface composition of coagulants before and after coagulation studies [50]. Since PACTPPg is a newly developed and not yet a published coagulant, the morphology and

surface composition analysis is essential in this study. A small volume of all types of coagulants was used to observe its characteristics for a comparison purpose using both dry and wet methods. The morphology of PACTPPg was analysed using the standard method of ASTM E1508 and the wet method of SEM-EDX using the Cryo technique. Cryo SEM is a standard method of examining solid and liquid specimens by imaging them at near liquid nitrogen temperatures. The wet method was done because the original form of PACTPPg was liquid after combining and dissolving both of the coagulants. Then, SEM images were taken at various magnifications. After that, the measurement of EDX was done to detect the significant elements in the coagulant. The images were obtained using a Zeiss EVO LS10 (Germany) instrument model.

2.3.3 Fourier transform infrared (FTIR) spectroscopy

The analysis of FTIR was performed to determine the present unique composite spectra, to observe the functional groups and the composition of coagulants using PerkinElmer Spectrum 100 model (USA), following the standard method of ASTM E168. It allows speedy analysis of a wide range of samples, from liquids to hard solids. The dried form of each type of coagulants was used, and the samples were dried in the laboratory vacuum oven at 40 °C for 24 hours for this analysis [11]. The FTIR spectra would be recorded in the range of 4000-600 cm^{-1} using the spectrophotometer instrument.

2.3.4 X-ray diffraction (XRD) spectrometry

XRD analysis was used to investigate further the composition of PACTPPg, PAC and TPP, coagulants using Bruker D8-Discover (USA) instrument with the standard methods of ASTM D5357 using Bragg-Brentano Diffractometer. Generally, XRD is used in this study to determine and observe the crystalline phases of elements in the samples in the range of 2 thetas (θ) scale of 0–90° angle with Cu-Ka radiation [14]. Diffracted intensity versus 2θ is recorded by a point or a small linear detector. The other key roles of this analysis is to determine the possibly unique existing compounds through qualitative phase analysis as well as structure determination and refinement. Specific amounts of samples were prepared and dried and kept in the desiccator until the day-analysis.

2.3.5 Zeta (ζ) potential, particle size, conductivity

The measurement of ζ potential was conducted to determine the existence

charges of colloidal particles in the optimum conditions of prepared coagulant samples using the technique of dynamic light scattering of Malvern Zetasizer Nano ZSP instrument (UK). A small amount of liquid sample was drawn and immediately measured for the ζ potential with the millivolts (mV) unit with the standard method of ASTM E2865. The coagulant samples needed to be freshly prepared to elude the irrelevant results. By using the same instrument, the parameters of particle size with the standard method of ASTM D422 and conductivity with the standard method of ASTM D1125 could also be determined in the units of diameter values in nanometers (d.nm) and millisiemens per centimetre (mS/cm), respectively.

2.3.6 Isoelectric point

The isoelectric point is the point where the charge of the coagulants is zero or balance between positive and negative at a certain pH. By referring to the pH value at the isoelectric point, the optimum pH during coagulation and the trend of coagulation efficiency can be predicted [25]. Each coagulant would have its isoelectric point value. Isoelectric point analysis was conducted to study the behaviour of PACTPPg under different pH values (3 to 10). Furthermore, by using the isoelectric point, the optimum pH of coagulant could be predicted. The measurement procedures for the isoelectric point was based on Lo [53]. The Malvern Zetasizer Nano ZSP was used to measure isoelectric point that corresponding to the value of ζ potential, using the standard titration method of acid and base in this study. The analysis was repeated with other types of coagulants as well.

2.3.7 Molecular weight

The measurement of molecular weight was done as well by using Malvern Zetasizer Nano ZSP in the kilodalton (kDa) unit following the standard method of ASTM D5296, which was done by a competent laboratory engineer. However, the international system (SI) unit was used in this study by converting it to g/mol. The optimum weight ratio solution of PACTPPg using RSM optimisation was tested for its molecular weight properties. The other different concentrations of coagulant solutions (PAC, TPP, and PAC+TPP) were tested as well. The information regarding molecular weight is essential as it helps the floc formation during the flocculation step.

3. Results And Discussion

3.1 Development and characterisation of composite coagulant

This section discusses the results regarding the development of finding the optimum composite coagulant of PACTPPg. The first stage of PACTPPg development is the combination of both coagulants of PAC and TPP as described in the methodology according to different weight ratios (Table 2). The best weight ratio of TPP/Al was determined based on the coagulation performance of the coagulant in treating leachate sample. This section also presents the structure, morphological, and physicochemical characteristics of PAC and TPP to further understand the properties of PACTPPg. Some analyses of PAC and TPP were characterised using its original powder form, i.e., Fourier-transform infrared (FTIR) spectroscopy and X-ray diffraction (XRD). Meanwhile, scanning electron microscopy/energy-dispersive X-ray (SEM-EDX), pH, ζ potential, isoelectric point, molecular weight, particle size, and conductivity tests were performed using its liquid form after dissolving the coagulants at the respective concentrations. Similar characterisation tests were also performed on the optimum PACTPPg. Before further discussions regarding the composite coagulant, the individual coagulants of PAC and TPP were analysed first to determine their best properties in the synthesis of PACTPPg.

3.1.1 Structure and morphological characteristics of PAC and TPP

The characteristics of PAC and TPP coagulants are discussed in this study in terms of physical-chemical properties, structure, and morphology. For the structure and morphological characterisation, 10% concentration of PAC was prepared and analysed quickly using the wet method of the SEM-EDX instrument. The analysis needs to be done immediately because PAC tends to dilute quickly in distilled water, which would likely result in an idle image. Figure 2 shows the appearance of 10% PAC at 300× magnification. Based on the observation, it shows that PAC has a long-connected structure like polydimethyldiallylammonium chloride (PDM) in (Appendix), which is likely to portray its polymeric chain properties with a mean diameter of 41.3 µm. It also has heterogeneous shapes deposited on the surface, which might be the reason for the uneven appearance. The state of PAC here also represents a non-compact texture by showing such void spaces surround the polymer (Figure 2). By using EDX, chlorine (Cl), sodium (Na), nitrogen (N), and aluminium (Al) were detected on the surface particles of PAC with respective weight and atomic percentages (Appendix). Based on the observation of the EDX spectrum, there are two noticeable elements found in PAC, i.e., Cl and Na.

Next, the SEM-EDX analysis was done on the TPP coagulant. It could be observed that the image of TPP had distinct differences from the PAC coagulant. The morphologies of 1% TPP solution and raw TPP are depicted in Figures 3 and 4, respectively. Figure 3 illustrates the liquid form with 150× magnification. It was observed that the TPP solution has fibrous-like characteristics, much likely to resemble its sticky and adhesive properties with a mean strand size of 241.5 µm. The morphology of tapioca peel in the study is virtually similar to the tapioca starch solution as studied by Azizan [50] (Appendix). However, a lower contribution of fibrous components and strands could be observed. The less fibrous component is due to the less starch content in the peels compared to the starch from the root tuber itself. Small particles were also deposited on the strands (yellow circles) that depicted the undissolved starch of TPP, which resulted in fewer strands. Figure 4 shows the image of raw TPP coagulant with 3,000× magnification. Based on the observation of the image, TPP exhibits smooth globular particles and polygonal-shaped starch granules in the form of agglomerated particles with a mean diameter of 9.0 µm. This occurrence is in good agreement with the previous findings by Versino *et al.* [37] and Shaylinda [25], who studied the morphological observation on the raw tapioca starch (Appendix). This result verifies that the morphological structure of the starch extracted from the agro-waste of tapioca peel is almost similar to the starch from the tapioca tuber.

The surface morphologies of starch are usually in granule shape, solid surface, and non-pores. However, they are distinguishable from the perspective of particle size distribution according to a comparison study done by Choy *et al.* [19] on the starch of rice, wheat, corn, and potato. The images obtained for TPP in the current work are also found to be in close agreement with the

characterisation of cassava peel reported by Asharuddin *et al.* [44]. Consequently, several elements could be found on the surface of TPP particles through EDX (Appendix). Several elements were noticeable, including carbon (C), iron (Fe), calcium (Ca), and Al. Silica (Si) and potassium (K) were also discovered, but in the slight amount (Appendix). The properties of Si could promote the coagulating process by accelerating the precipitation formation [17, 44]. Besides, the content of Si particles would trigger the coagulant to perform effectively, which is achieved by inducing the ionic exchange and heteroaggregation of oppositely charged colloids in wastewater [54].

Further analysis was done to evaluate the structural bonding formation of both PAC and TPP coagulants. In this study, FTIR spectroscopy was used to investigate the bonding characteristics by examining the present spectral bands. According to Kakoi *et al.* [55], pollutant removal could depend on the ionisation degree of the functional groups of the polymer structure in the added coagulants. The main identified spectral bands of both PAC and TPP are shown in Tables 3 and 4, respectively, whereas the extensive analysis is available in the Appendix. According to Versino *et al.* [37], FTIR spectroscopy could reflect the changes of spectral band characteristics, which resemble the physical and chemical interactions when two or more substances are synergised together. Therefore, the potential interactions between PAC and TPP are expected in this study. The spectral bands of raw PAC and TPP were observed individually for comparison purpose. Meanwhile, further discussions of FTIR results for the composite coagulant PACTPP are presented in section 3.2.1. Figure 5 shows the FTIR spectra of raw PAC and TPP coagulants.

Based on the infrared spectral database (Appendix), the IR spectra of PAC show that strong absorption bands could be observed in several regions, which indicated particular functional groups. A very broad intensity was detected at 2500-3100 cm^{-1} (i.e., specifically at 3013.07 cm^{-1}), which denoted the existence of carboxylic acid compounds with O-H hydrogen-bonded stretching. Furthermore, alkenes and aromatic ring compounds with C=C-H asymmetric stretching could also be identified (Table 3). The characteristics of C≡C stretching vibration could be observed as well at the wavenumber of 2163.44 cm^{-1} in the 2260−2100 cm^{-1} absorption range. Moreover, the peak wavenumber at 1635.14 cm^{-1} might belong to several compounds, such as alkenes, aldehydes, amines-primary, and amides with respective stretching vibrations and bends (Table 3). The strong intensity of C-O stretching was also detected at 1050−1150 cm^{-1} absorption range with 1097.96 cm^{-1} as the peak wavenumber that resembled the alcohol compound. Other than that, a strong and broad band with 1097.96 cm^{-1} peak was observed at the range of 1110−1000 cm^{-1}, which could be related to the silicate compound and the asymmetric stretching vibration of Al-OH-Al [11]. According to Yang *et al.* [11], the peaks of 557 cm^{-1} and 975 cm^{-1} are also related to Al-O vibration and Al-OH-Al stretching, respectively, in the spectra of PAC.

Table 3 Main functional groups of PAC from FTIR spectrum analysis

Functional Group	Absorption Range (cm^{-1})	Vibration Type
Carboxylic Acids	3100−2500	O-H stretching
Alkenes	3100−3000	C=C-H asymmetric stretching
	1675−1600	C-C=C symmetric stretching
	1680−1620	C=C non-conjugated
Aromatic Rings	3100−3000	C=C-H asymmetric stretching
Alkynes	2260−2100	C-C≡C-C
Aldehydes	1750−1625	C=O stretching
	1750−1590	C=O conjugated
Amines-Primary	1640−1560	N-H bending
Amides	1670−1600	C=O stretching
	1640−1550	N-H bending
Alcohols	1150-1050	C-O stretching
Silicates	1110−1000	Si-OR stretching, asymmetric stretching vibration of Al-OH-Al

More chemical groups and bonds could be observed following respective wavenumbers (cm^{-1}) in TPP compared to PAC (Table 4 and Appendix). The broad band of 3500−3200 cm^{-1} with the peak at 3275.75 cm^{-1} might be allocated to the O-H group in polymeric compounds, e.g., carboxylic acids, phenols, and alcohols, as well as the O-H group of free hydroxyl groups existed in the peel [44]. The peaks at both wavelengths between 3200−3300 cm^{-1} and 2100−2260 cm^{-1} with 3275.75 cm^{-1} and 2168.01 cm^{-1}, respectively, indicated a similar group of alkyne compounds with different types of vibration. The strong intensity was identified in ≡C-H stretching in the CH stretching, whereas the medium intensity was observed in the -C≡C- of C≡ stretching vibration. The H-C-H asymmetric and symmetric stretching might also be found in the 2850−2960 cm^{-1} range that belonged to the alkanes of alkyl groups with the peak wavenumber of 2931.24 cm^{-1}. Another main group existed that built up the structure of TPP was identified in alkene compounds with non-conjugated C=C bending, which was reflected in the wavelength of 1620−1680 cm^{-1} (i.e., specifically, the peak at 1640.37 cm^{-1}). The peak at the wavenumber of 1640.37 cm^{-1} might also belong to the amines-primary group with the N-H bend stretching found in PAC as well.

Table 4 Main functional groups of TPP from FTIR spectrum analysis

Functional Group	Absorption Range (cm^{-1})	Vibration Type
Alkynes	3300−3200	≡C-H stretching, CH stretching vibrations
	2260−2100	C≡ stretching, -C≡C-
Alkanes, Alkyl Groups	2960−2850	C-H, H-C-H asymmetric and symmetric stretching
Carboxyl	1750−1680	C=O stretching
Alkenes	1680−1620	C=C non-conjugated
Amines-Primary	1640−1560	N-H bend stretching
Alcohols	1300−1000	C-O stretching, −COOH
	1150−1050	C-O stretching
Silicates	1110−1000	Si-OR stretch, asymmetric stretching
Secondary Cyclic Alcohols	990−1060	C-OH stretching
Alkyl Halides	600−800	C-Cl stretching

The alcohol structures found in PAC were also identified in TPP, with both peak wavenumbers at 1077.04 cm^{-1} and 1103.78 cm^{-1}, respectively. Besides the alcohol compound, the secondary cyclic alcohol compound was also observed in the absorption range of 990−1060 cm^{-1}, with 998.73 cm^{-1} peak wavenumber. The bonds related to silicate compounds were also observed at the peaks of 1077.04 cm^{-1} and 1103.78 cm^{-1} in the range of 1110−1000 cm^{-1} [11]. Meanwhile, the deep peaks observed between 600 and 800 cm^{-1} indicated the C-Cl stretching of alkyl halide compounds through two identified peak wavenumbers at 763.29 cm^{-1} and 706.86 cm^{-1}, respectively, with strong intensity. According to Chen *et al.* [15], the discovered peaks in the range of 1077.04−1103.78 cm^{-1} could be attributed to the asymmetric stretching vibration of Fe-OH-Fe or Al-OH-Al. Meanwhile, the bending vibration of Si-O-Al or Si-O-Fe bonds might exist due to the peaks that appeared around 998.73 cm^{-1} [15]. The results and trends obtained for the wavenumbers of TPP are also in agreement with the characterisation studies of tapioca peel using FTIR analysis by Asharuddin *et al.* [44]. The structural properties of TPP are also almost similar to other natural peels, such as citrus and mango peels [44].

Hydroxyl (O-H), hydrogen bonding, carboxyl (C=O), amino, or amide (-NH$_2$) groups are also the preferred groups for the coagulation-flocculation process. At the wavelength range of 3500−3200 cm^{-1}, the bonded O-H in polymeric compounds, e.g., alcohol, carboxylic acids, phenols, and O-H groups of free hydroxyl groups might present to induce the flocculating activity [44]. The identified groups are in agreement with the FTIR analysis done on watermelon seeds [57], banana pith [55], and *Cecropia obtusifolia* seeds [58] for the coagulating features, as shown in Table 5. Misau & Yusuf [58] studied the coagulant properties of crushed watermelon seeds and concluded that the presence of proteins observed through the spectra of 3447, 1845, 1740, 1647, 1559, 1541, and 1419 cm^{-1} helped in the water treatment (Table 5). The existence of protein properties in a coagulant is beneficial in order for the coagulant to work efficiently as the proteins behave like silica elements that help in the destabilisation mechanism, as reported by Fatombi *et al.* [54] who developed a coagulant from the extract of *Cocos nucifera* for water purification. According to Shak & Wu [58], broader and fewer absorption bands would be found in inorganic coagulants compared to narrower and intense bands in organic compounds, which resulted in more absorption bands. This outcome supports that the bigger range of wavelength numbers would enhance the

potential of natural materials to facilitate more contaminant removal in water treatment, as claimed by the study of Kakoi *et al.* [55] who used banana pith powder.

Banana pith had proven the potential to treat turbid water by removing 98.5%, 54.3%, 96.03%, 98.9%, 88.7%, 100%, 100%, 92%, 81%, 100%, and 60% of turbidity, COD, suspended solids, sulphates, nitrates, Cu, Cr, Fe, Zn, Pb, and Mn, respectively [55]. Another study that used banana peel indicated that the functional groups, i.e., the carboxylic acid (C=O), hydroxyl (-OH), and aliphatic amines (N–H), showed both positively and negatively charged species [56]. These groups might promote the charge neutralisation mechanism by neutralising the negative impurity charge in the leachate sample. On the other hand, in a study done by Shak & Wu [58], the functional groups of O-H stretching, CH_2 groups in fatty acids (i.e., symmetrical and asymmetrical stretching), and C=O stretching in *C. obtusifolia* seed were identified as the coagulating agents to help in the removal of 87% suspended solids and 55% COD. In conclusion, from the structure and morphological characterisation studies of PAC and TPP, it is proven that both materials have coagulating properties, especially for TPP as a newly-discovered natural coagulant. Table 5 shows the FTIR analysis of natural materials in water treatment and its detection in TPP.

Table 5 Functional groups identified in several natural materials

Natural Materials	Absorption Range/ Wavelength Number (cm^{-1})	Identified Functional Groups	Detected/Not Detected (N.D.) in TPP
Watermelon Seeds [57]	3770−3650	AlO-H stretching vibration	N.D.
	3447.68	N-H group stretching	N.D.
	2930−2820 (2925.49 & 2854.13)	CH$_2$ asymmetric stretching CH$_2$ symmetric stretching	Detected
	2360.54	Si-H (silane)	Detected
	1845.28	C=O (5-membered β-lactones)	N.D.
	1740.89	C=O (Carboxyl)	Detected
	1654.27	−C=C− symmetric stretching of alkenes	Detected
	1647.87	N-H bending (1° amines)	Detected
Banana Pith [55]	3369.4	O-H group vibration	Detected
	2925.8	C-H stretching	Detected
	1645	Asymmetric stretching, carboxylic COO-double bond, deprotonated carboxylate	Detected
	1384.8	Symmetrical or asymmetrical stretching of ionic carboxylic groups (COOH), pectin	Detected
	1247	C-O stretching of ketones, aldehydes, and lactones or carboxyl groups	Detected
	1029.9	-C-O-C and -OH of polysaccharides	Detected
	848.6	Amine groups	Detected
C. obtusifolia Seeds [58]	3281	O-H stretching	Detected
	2923 & 2853	CH$_2$ groups in fatty acids (symmetrical and asymmetrical stretching of C-H)	Detected
	1800 & 1600	C=O bond stretching	Detected

3.1.2 Physicochemical characteristics of PAC and TPP

For the physical and chemical characteristics of respective coagulants, 10% PAC and 1% TPP were analysed in their liquid form. These characteristics are essential to analyse as they have major control over the particles' surface charges and polyelectrolyte charge density. Table 6 shows the results of physicochemical characteristics in terms of pH, ζ potential, isoelectric point, molecular weight, particle size, and conductivity parameters. Based on the observation, these findings verified that PAC has the acidic properties with pH 3.36 and high ζ potential value at +20.5 mV. The determination of ζ potential is essential to confirm the role of the charge neutralisation mechanism [59]. A higher ζ potential would be beneficial for better coagulation performance due to the superior charge neutralisation process taking place [60, 61].

The disseminated PAC coagulant during the treatment process would neutralise the stabilised negative particles (-18.73 mV) of raw leachate effectively, as discussed earlier in section 4.2. On the contrary, the TPP solution practically has a neutral feature with pH 6.33 and negative ζ potential value at -0.68 mV. This result shows an agreement with other starch-based coagulants that have approximate pH and ζ potential values in previous studies [62]. Based on the findings of Azizan [50], the ζ potential of tapioca starch was -0.559 mV with pH 6.8, whereas Ong [63] discovered the ζ potential values of -3.12 mV for tapioca flour and -4.37 mV for sago starch. Similarly, the use of psyllium husk and tobacco leaf as the primary coagulant and coagulant aid showed high negative charges of -1.92 and -3.57 mV as identified by Al-Hamadani *et al.* [61] and Rusdizal *et al.* [62], respectively.

Table 6 Physicochemical characteristics of PAC and TPP

Coagulant	pH	ζ Potential (mV)	Isoelectric Point (pH)	Conductivity (mS/cm)	Molecular Weight (g/mol)	Particle Size (d.nm)
PAC (10%)	pH 3.36	+20.5	pH 8.90	71.5	8.55×10^4	6.152×10^2
TPP (1%)	pH 6.33	-0.68	pH 7.25	0.786	5.67×10^6	4.079×10^4

The low ζ potential also indicates that tapioca is polymerised-anionic carbohydrates that have carboxylic substitutions [64]. The low ζ potential of TPP would cause low capability in neutralising the colloids of the same-charged leachate particles. In this case, it also would cause the charge reduction in PACTPP as PAC would combine with TPP that has a low negative charge. However, the addition of TPP polymer with higher molecular weight (5.67×10^6 g/mol) and bigger particle size (4.079×10^4 d.nm) would help to cater the weakness of PAC to become more dense and compact. TPP as a starch-based coagulant can also perform coagulation by charge neutralisation to remove any positively charged pollutants and accomplish sweep flocculation through the adsorption-bridging mechanism during treatment [65]. Subsequently, the isoelectric point is interrelated with the parameters as mentioned earlier. The ζ potentials of 0 mV in PAC and TPP coagulants were determined at pH 8.90 and pH 7.25, respectively.

The isoelectric point of TPP also shows the agreement with previous research of natural coagulant extracted from *C. Nucifera* at pH 7.5, as studied by Fatombi *et al.* [54]. The identification of ζ potential and isoelectric point provides some ideas on the conditions of coagulants to work effectively during the treatment process.

Meanwhile, on the conductivity parameter, PAC is characterised with high value that portrays its capability of flowing electric current compared to TPP, which is due to the concentrations of cations and anions, as well as dissolved inorganic constituents [66]. Despite the superiority of PAC, TPP is dominant in terms of molecular weight and particle size of 5.67×10^6 g/mol and 4.079×10^4 d.nm, respectively. These properties show that the presence of TPP could complement the disadvantages of PAC to become an effective coagulant [67, 68]. Oladoja [59] also stated that the operation of natural polymeric coagulants could predominantly occur via the adsorption-bridging mechanism, where its molecular weight needs to be distinctively high to perform efficiently. Next, the physical and chemical characterisation was continued with the analysis of XRD for the determination of crystalline phases in the solid coagulants.

In PAC, the tridecamer of Al_{13} or $AlO_4Al_{12}(OH)_{24}^{7+}$ is widely reported to be the most efficient and predominant species due to its higher positive charge among others: the monomers Al^{3+}, $Al(OH)^{2+}$, $Al(OH)^{2+}$, $Al(OH)_{3(am)}$, and $Al(OH)^{4-}$, a dimmer ($Al_2(OH)^{24+}$), and a trimer ($Al_3(OH)^{45+}$) [69, 70]. Nevertheless, the peak of Al_{13} species in PAC products could not be proven without any modification; therefore, it needs respective reagents to separate the Al_{13} precipitate [50]. High-purity Al_{13} products could be obtained by using sulphate precipitation and consequent barium nitrate metathesis operations or the SO_4^{2-}/Ba^{2+} deposition-replacement method from the medium-high concentration of PAC [69, 71]. The result for XRD analysis is presented through the peaks that occurred from the analysis spectra. Figure 6 displays the spectra of raw PAC coagulant in the range of 2-theta (θ) scale.

Based on the observation in Figure 6, strong crystalline peaks are detected at the angle of 15°, 17°, 18°, 23°, 24°, 25°, 26°, 27°, 28°, 30°, 31°, 32°, 33°, 35°, 39°, 42°, 44°, 47°, 50°, and 52°, which possibly present the bonding of aluminium chloride hexahydrate ($AlCl_3 6H_2O$) [72]. The pattern of raw PAC here could be noted as semi-porous and irregular, which resembled its unwell-formed

crystalline structure, unlike the Al_{13}-(SO4)n precipitate that primarily consists of well-formed crystalline solid when analysed by ^{27}Al-NMR spectroscopy [71]. The characteristic of well-formed crystalline solid is due to the separation and purification processes that cause the precipitate to contain more Al_{13} than PAC itself. Despite the difficulty in detecting this main species, some studies stated that a strong Al_{13} signal could appear in the range of 2θ from 5° to 25° of low angles in the XRD spectrum of the original PAC [69]. Thus, through the characterisation by using XRD, it could be described that PAC has the semi-formed crystalline phase. Nonetheless, PAC contains highly charged positive atoms, which made PAC as the preferred inorganic polymer coagulant. Next, the raw TPP was also characterised to determine its physicochemical properties by using XRD. The spectral pattern of TPP is presented in Figure 7. Based on the observations, the XRD of the starch shows non-sharp peaks at low angles of 2θ, at 15°, 17°, 18°, 19°, and 23°, respectively.

Based on the obtained curve fitting routine and finding areas under the curve for each group, the components such as potassium iron silicate ($K_2Fe_2Si_{0.29}O_{4.58}$), aluminium potassium silicon ($K_8Al_{8.02}Si_{37.98}$), and silicon oxide (SiO_2) were distinctly detected in the analysis. The distinct peaks could be observed from starch-based materials if the element is crystalline, which would reveal a certain extent of particle uniformity as a biopolymer. In general, all starch could be classified as low crystalline polymers with sharp crystalline peaks that are visible across the same region of 10°–30° [73]. The spectra in Figure 7 also consists of broad patterns (25°–60°) without any distinguished sharp peaks that indicate its amorphous properties in nature [74]. These findings are in line with the study done by Oladayo *et al.* [74] that investigated the properties of biofilms prepared using cassava starch and starch-keratin blend. Comparisons were also made with the diffraction peaks obtained by the starch of potato, corn, wheat, and rice [73], and tapioca starch [50], which showed similar patterns of the graph (Appendix). By referring to the spectra obtained, it could be noted that tuber-based starch has lower particle uniformities according to the lower percentage of crystallinity compared to cereal-based starch. In this study, the tapioca peel was obtained from the tapioca tuber itself; therefore, it could be concluded that its level of crystallinity is also minimal.

The low crystallinity level might also be attributable to the high polymerisation of amylose molecules and a small presence of proteins and lipids in the composition of TPP [73]. The results from this characterisation are also in agreement with the study done by Zayadi *et al.* [47], in which the pattern of diffraction peaks in natural materials appeared within the same curve area of low angles. In the study of Zayadi *et al.* [47], the potential of agro-wastes, i.e., cassava peel, banana peel, and coconut coir as the medium for metal and nutrient removals were investigated. Cassava peel was chosen as the promising natural material as most of the significant compounds were discovered at the foremost diffraction peaks (Table 7). However, the cassava peel here was prepared without discarding the outer brownish layer, which might attribute to the dissimilar compound obtained. Table 7 shows the significant compounds found in the cassava peel in comparison with TPP according to its peaks. Overall, it could be concluded that TPP has major amorphous properties, in which the crystallinity of the starch might not give much impact on the treatment performance if used as a primary coagulant [73].

Table 7 Comparison of compounds based on XRD peaks on cassava peel and TPP in this study

Agro-waste	Peak (°)	Compound	Agro-waste	Peak (°)	Compound
Cassava Peel [47]	15°	Iron chloride hydrate	Tapioca peel powder (TPP)	15°	Potassium iron Silicate ($K_2Fe_2SiO._{29}O_{4\cdot58}$)
	17°	Diosgenin		17°	Siderite ($Fe(CO_3)$)
		L-lactide-poly (ethylene glycol)		18°	Calcium aluminium silicide (CaAlSi)
		4-chlorophenyl sulfone		19°/23°	Aluminium potassium silicon ($K_8Al_8.O_2Si_{37\cdot98}$)
	17°/23°	Starch (maize)		26°	Carbon (C)
	26°	Carbon		27°	Silicon oxide (SiO_2)
	27°	Diclone			
		Silicon oxide			

3.2 Characterisation of composite coagulant (PACTPPg)

The conventional coagulation-flocculation treatment of landfill leachate had been done earlier using all the prepared different weight ratios of composite coagulants. Based on the observation, PACTPPg has been designated as the best optimum weight ratio according to the obtained removal percentages. In this section, the study of PACTPPg is emphasised by examining its structure, morphology, physical, and chemical characteristics using SEM-EDX, FTIR, XRD, pH, ζ potential, isoelectric point, molecular weight, particle size, and conductivity analyses.

3.2.1 Structure and morphological characteristics of PACTPPg

Morphological property is an in-depth key parameter for the visual analysis of a composite material [17]. In complementary to the morphological characteristics of individual PAC and TPP, PACTPPg is considered as the combination of both coagulants, as could be seen in Figure 8. In brief, these characteristics are evidence of a favourable composition process to develop a new coagulant. Figure 8 exhibits the SEM image of the PACTPPg solution of TPP/Al = 3.71 with 200× magnification. It is observed that the coagulant has heterogeneous and uneven shapes with a bigger mean size of 142.3 μm, which could increase the surface area to initiate more spots for the adsorption-bridging between particles to take place [17]. The increment of size is about 70.1% compared to the PAC solution with 300× magnification in the earlier analysis (section 3.1.1). PACTPPg also shows a further compact and occupied state of coagulant, which occurs due to the addition of TPP that has altered PAC in the new present form. The longer-connected and multi-branched structure describing the fibrous properties originated from TPP has also been discovered in PACTPPg. The multi-branched structure formed does not only contribute to larger fractal dimension and size of the polymer but would also improve the bridging effects and the aggregating abilities [17, 58, 75].

Next, the EDX analysis was done to identify the elemental compositions of PACTPPg. The EDX recorded the elements, i.e., carbon (C), aluminium (Al), silica (Si), chlorine (Cl), potassium (K), sodium (Na), calcium (Ca), and iron (Fe) on the surface of PACTPPg's particles. Based on the observation of the EDX spectrum, C has the notable increment compared to the C element found in PAC, which resulted from the addition of organic substance throughout the process. These results also conclude that the addition of TPP increased the weight of some elements in the new PACTPPg. Furthermore, Niu *et al.* [76] and Zhu *et al.* [77] stated that the increase of polymerisation degree to form polymer chains or three-dimensional networks would improve the stability of the composite coagulant. The formation of macromolecular compounds, such as Al-O-Si or Al-Si-Fe complexes, might be responsible for the better performance of PACTPP [6, 76]

Previously, the FTIR analysis was done on the sole coagulants of PAC and TPP. Based on the results, it is noted that the existed dominant functional groups would help in the coagulation-flocculation process. TPP also showed such exceptional characteristics that proved the capability of the natural coagulant developed from agro-waste. FTIR analysis was also done on PACTPPg to

examine the information of conceivable inter- or intramolecular interaction in the compound through the molecular geometry and functional groups [37, 78]. According to the wavenumber analysis in PACTPPg, various chemical groups and bonds could be detected, including the new groups that did not appear in the individual PAC and TPP coagulants. The main identified spectral bands are shown in Figure 9 and Table 8, where the extensive analysis could be viewed in Appendix.

Based on the observation in Figure 9, it is clear that the spectrum of PACTPPg is slightly similar to TPP but not the complete combination of PAC and TPP spectra, which has broader and denser intense bands, especially in the range of 3500−2500 cm^{-1}. The broader and denser intense band is due to the intermolecular stretching vibration of dissociative −OH [9, 13, 75], since PACTPPg was prepared through the dilution of PAC and TPP in distilled water, and then dried for the adsorption spectrum analysis. The functional group consists of −OH is one of the important factors to indicate the efficiency of coagulants [13]. Next, it is observed that the peak of 3231.46 cm^{-1} belongs to the wide-ranging bands of 3600−3100 cm^{-1} and 3500−3100 cm^{-1} that respectively assigned to alcohols, phenols, and amines-secondary functional groups [25, 44], which appear with strong O-H stretching and medium N-H bend intensities, respectively. Compared to PAC and TPP, some adsorption bands, i.e., the chemical bonding of carboxylic acids (3400−2400 cm^{-1}) with peaks at 3231.46 cm^{-1}, 2518.62 cm^{-1}, and 2511.76 cm^{-1}, the bonding of alkenes (1675−1600 cm^{-1}), and amines-primary (1640−1560 cm^{-1}) with a peak at 1629.79 cm^{-1} also existed [11]. Table 8 shows the main functional groups of PACTPPg from FTIR spectra analysis.

Table 8 Main functional groups of PACTPPg from FTIR spectra analysis

Functional Group	Absorption Range (cm^{-1})	Vibration Type
Alcohols, Phenols	3600−3100	Hydrogen-bonded O-H stretching Strong and broad intensity
Amines-secondary	3500−3100	N-H bending Medium intensity
Carboxylic acids	3400−2400	Hydrogen-bonded O-H stretching
	3300−2500	O-H stretching Medium intensity
Ketones	1750−1625	C=O Newly discovered group
Aldehydes	1750−1625	C=O Newly discovered group
Alkenes	1675−1600	C-C=C symmetric stretching Medium intensity
Amines-primary	1640−1560	N-H bending Medium intensity
Alkanes	1370−1350	C-H rocking mode Newly discovered group Medium intensity
Phosphates	1200−1100	P=O stretching Strong intensity
Silicates	1110−1000	Si-OR stretching Strong and broad intensity

The carboxylic acid group has the same stretching vibration as alcohols-phenols, which is hydrogen −OH. Despite the bending of water adsorbed, it could be considered that PACTPPg contained more absorbed, crystallised, and polymerised water than others by having stronger intensity peaks. It is also an essential factor for coagulants to work effectively [8, 15]. The intensity peaks of PACTPPg are also stronger than PAC and TPP coagulants, which indicate that the coagulant consists more free radical form of dissociative −OH [11, 15]. Other than that, the existence of bonding groups of alcohol-phenols (3600−3100 cm^{-1}), amines-secondary (3500−3100 cm^{-1}), 1°-2° amines amides (3400−3250 cm^{-1}), aromatics (1500−1400 cm^{-1}), sulphates (1450−1350 cm^{-1}), nitro groups (1400−1300 cm^{-1}), alkyl halides (1300−1150 cm^{-1}), and phosphates (1200−1100 cm^{-1}), as presented in Table 8 and Appendix were observed due to the absorption bands of the groups that appeared only in TPP. Meanwhile, only two functional groups observed due to the source of PAC, i.e., amines-primary (1640−1560 cm^{-1}) and amides (1640−1550 cm^{-1}), with the same peak at 1629.79 cm^{-1}. The amines-primary and amides groups respectively indicate the similar type of vibration of N-H bending with medium intensity.

Next, near the 1400 cm^{-1} wavelength, the absorption peaks appeared on PACTPPg and TPP, but it did not appear in PAC. According to Chen *et al*. [13], who developed a new composite coagulant of polyferric-aluminium-silicate-sulphate, it could be deduced that the peaks were assigned to Al-O-Al bond stretching and bending vibration. Simultaneously, the peaks between 1359.32 and 1151.24 cm^{-1} (Appendix) could indicate the sign of Si-O-Si bonds [9]. Silicate stretching (Si-OR) with a strong and broad intensity was also determined in the ranging band of 1110−1000 cm^{-1}, with the discovered peaks at both 1078.08 cm^{-1} and 1018.07 cm^{-1}. Phosphate stretching (P=O) was also discovered at the peak of 1151.24 cm^{-1}. Meanwhile, in the region of 1125−1000 cm^{-1}, the spectra of PACTPPg were almost similar to the TPP spectra. Besides, it could be noted that the addition of heated TPP did not diminish the existence of the main bonds in PAC, e.g., carboxyl, amine, and amide that helped in the coagulating process [25]. Other additional bonds of C-O bonds probably existed as well when the compositing process had started. According to Shaylinda [25], the C-O bonds were highly detected in the spectra of tapioca starch, which could stimulate the new bonds in PACTPPg.

The remarkable findings in the analysis of PACTPPg could happen due to the peaks that appeared around 1750−1625 cm^{-1} and 1370−1350 cm^{-1}, which are unobservable in TPP and PAC spectra. According to these experimental findings, it could be suggested that some new chemical compounds, probably from the functional groups of ketones (C=O), aldehydes (C=O), and alkanes (C-H rock) formed when heated TPP was introduced into PAC, as shown in Figure 9 and the highlighted row of Table 8. The new chemical compounds indirectly indicate that PACTPPg did not just involve a simple physical mixing, but also the chemical synthesis with some reactions occurred between these two coagulants [10, 14].

3.2.2 Physicochemical characteristics of PACTPPg

Regardless of PACTPPg: TPP/Al = 3.71 becomes the optimum composite coagulant, physical and chemical characterisation tests were carried on all ten ratios of PACTPP to observe their properties in becoming the ideal coagulant for the treatment of raw stabilised leachate. Table 9 shows the properties of different weight ratios of PACTPP (a−j) in terms of pH, ζ potential, particle size, and conductivity parameters. It could be seen that the addition of TPP into PAC during the composite process affected the outcome solution. It was noted that TPP/Al = 64.94 had the lowest values of ζ potential and conductivity at +1.81 mV and 9.13 mS/cm, respectively, and the biggest particle size of 6.019 × 10^4 d.nm. These properties are certainly contributed by the utmost amount of TPP in PACTPPa that has the highest molecular weight. Combining polymerised coagulants with the higher molecular weight of anionic polyelectrolytes can enhance the aggregating ability of impurities during the treatment process [79]. The ζ potentials of PACTPP (a−j) also remained in the positively charged strength even though the particular amount of TPP had their anionic charges. This condition is favourable since the anionic polymer should have a weak anionic charge to hinder the weakening of the high-charge strength of the composite coagulant [25].

The decreasing ratio of TPP/Al from 64.94 to 0.65 increased the values of ζ potentials, decreased the size of particles, and improved the ability to pass an electric current through the measurement of conductivity in all final products of PACTPP. However, this is in contrast to the readings of the pH values in this characterisation study. Based on the results, all the developed composite coagulants are in the acidic condition, but not in the ascending nor descending orders until the end.

Table 9 Properties of different weight ratios of PACTPP (a−j)

PACTPP (a−j) TPP/Al	pH	ζ Potential (mV)	Particle Size (d.nm)	Conductivity (mS/cm)
a: 64.94	3.62	+1.81	6.019×10^4	9.13
b: 29.22	3.58	+2.24	5.909×10^4	12.15
c: 17.32	3.40	+2.67	5.801×10^4	15.17
d: 11.36	3.38	+3.10	5.693×10^4	18.20
e: 7.79	3.35	+3.22	5.304×10^4	22.30
f: 5.41	3.41	+3.33	4.916×10^4	26.40
g: 3.71	3.45	+3.45	4.528×10^4	30.50
h: 2.44	3.53	+3.52	4.029×10^4	32.57
i: 1.44	3.55	+3.59	3.532×10^4	34.64
j: 0.65	3.56	+3.66	3.035×10^4	36.70

Based on Table 9, it is observed that the pH values of PACTPP decreased from TPP/Al = 64.94 until TPP/Al = 7.79, and increased again at TPP/Al = 5.41 with pH 3.41 until TPP/Al = 0.65. The shift in pH certainly happened due to the changing point phase in weight ratio, where PAC started to have a higher proportion compared to TPP in PACTPPf. Next, regarding the satisfactory performance of PACTPPg, the molecular weight and isoelectric point tests were further done to emphasise its superiority. Table 10 displays the physical and chemical characteristics of PACTPPg in terms of pH, ζ potential, isoelectric point, molecular weight, particle size, and conductivity parameters, and also its comparison with PAC and TPP coagulants.

Table 10 Physicochemical characteristics of PACTPPg

Coagulant	pH	ζ Potential (mV)	Isoelectric Point (pH)	Conductivity (mS/cm)	Molecular weight (g/mol)	Particle Size (d.nm)
PACTPPg TPP/Al = 3.71	pH 3.45	+3.45	pH 9.81	31.5	1.59×10^7	4.528×10^4
PAC (10%)	pH 3.36	+20.5	pH 8.90	71.5	8.55×10^4	6.152×10^2
TPP (1%)	pH 6.33	-0.68	pH 7.25	0.786	5.67×10^6	4.079×10^4

Based on the findings in Table 10, PACTPPg was characterised by the acidic properties at pH 3.45, with a slight pH increase from the individual 10% PAC solution at pH 3.36. Meanwhile, a significant drop of ζ potential value was noticed in the PACTPPg compared to PAC by having a difference of 17.05 mV. Zeta potential studies are not just useful for the characterisation of particle surfaces, but also in the applications of determining the colloidal stability and in the ion adsorption studies [64]. Similarly, the addition of TPP into PAC also reduced the conductivity value of the composite coagulant. This brief conclusion is also in agreement as to the study by Shaylinda [25], who indicated that the low conductivity of heated tapioca flour altered the high conductivity of prehydrolysed iron coagulant during the composite process. Similarly, Moussas & Zouboulis [8] also recorded a massive reduction of conductivity value throughout the combination of polyacrylamide as a non-ionic polymer with polyferricsulphate. Therefore, it could be stated that the decline of conductivity of the final product is a typical outcome.

The isoelectric point test was also conducted on PACTPPg using the titration method. Based on the observation, the point where PACTPPg achieved 0 mV was at pH 9.81, PAC at pH 8.90, and TPP at pH 7.25. The relevance of result is supported by the previous findings in the study by Azizan [50] that also reported the increment of isoelectric point in its composite coagulant. As discussed earlier, the parameters of ζ potential and isoelectric point give the fundamental properties of coagulants' surface chemistry, which would further react during the adherence and contact with their surroundings [67]. These parameters affect the coagulation by counteracting the charges in raw leachate samples and give the expected optimum pH range to perform effectively [50]. However, based on the observation in the optimum pH (Appendix), the optimum pH range is between pH 4−7, which is much lower than the isoelectric point of PACTPPg at pH 9.81. The difference between the optimum pH and the isoelectric point happened due to the miscellaneous strength of positive charges of the composite coagulant (PACTPP (a−j)) compared to the raw leachate (-18.73 mV). For instance, the ζ potential of PACTPPa at +1.81 mV resulted in the optimum leachate pH for treatment at pH 4; meanwhile, PACTPPj was characterised with +3.66 mV and achieved the optimum leachate pH at pH 6.

Another equally important discovery is the increment of molecular weight and particle size of PACTPPg with 1.59×10^7 g/mol and 4.528×10^4 d.nm, respectively. The higher molecular weight of PACTPPg compared to PAC and TPP is the result of the convergence of both materials into a single product. This characteristic would enhance the aggregation capacity besides reducing the residual of aluminium concentration in the generated sludge [13]. Furthermore, the contact of the high molecular weight of coagulant and the linear structure of cationic organic matter with wastewater contaminants would result in the improved adsorption-bridging mechanism during coagulation-flocculation practice [14]. Teh *et al.* [67] also stated that the high molecular weight polymer could improve the aggregating ability via adsorption and bridging mechanism [67, 79].

The next characterisation test was the XRD analysis. The XRD spectra of PACTPPg as the composite coagulant is shown in Figure 10. There is a slight difference in the spectra between PACTPPg and PAC (Figure 6) and a distinct diffraction shift angle with TPP (Figure 7). As discussed previously, the spectra of PAC present the combination of both signs of crystallinity and irregular phase. Meanwhile, TPP shows no distinguished sharp peaks that indicate its amorphous properties in nature. Noticeably, the interpenetration of TPP has slightly altered the spectra pattern of PAC in generating PACTPPg. The newly generated composite coagulant was detected with several sharp and clear traces of crystal peaks around the angle of 15°−52°, as well as the broad and low intense peaks at 55°−90° of the diffraction angles. The distinct crystalline peaks were detected at 15°, 17°, 23°, 24°, 26°, 28°, 30°, 33°, 35°, 40°, 41°, 44°, 47°, 50°, and 52° that practically pose as the bonding of aluminium chloride hexahydrate ($AlCl_3 6H_2O$) [72]. Besides, based on the attained curve fitting routine of XRD spectra, the components of aluminium chloride hydroxide ($AlCl_3.6H_2O$), potassium aluminium chloride oxide ($KAlCl_2O$), chlormayenite ($Ca_{12}Al_{12}O_{32}C_{12}$), wadalite ($Ca_{12}(Al_{10.6}Si_{3.4}O_{32})Cl_{5.4}$), and potassium aluminium chloride silicate hydrate ($K_{12}Al_{10}Si_{10}O_{40}Cl_2.8H_2O$) were distinctly detected in the analysis (Appendix).

These polymeric complexes imply that to some extent, the introduction of TPP into PAC resulted in the formation of new compounds, which play an essential role in the stability and coagulation function [11, 13]. These compounds are shifted compared to the standard crystals, which is an indicator of lattice contraction or expansion according to the study of surface chemistry. The shifted compounds also could be the reason for the increment of the molecular weight of the product as discussed previously with 1.59×10^7 g/mol [11]. The abundance of characteristic peaks in the spectra data suggested that certain adsorbing chemical compounds existed [14]. Meanwhile, some of the detected compounds did not exist in the particular PAC and TPP, which demonstrated that PACTPPg is a novel polymer [14].

Furthermore, based on the spectral data, it is suggested that the existing polymeric hydroxide hydrate complexes that contain typical functional groups such as −OH, Al-OH-Al, Al-O-Al, Si-O, and Fe-OH-Fe play a significant role in the coagulation performance compared to the standard crystals [11, 13]. The broad and unrecognisable peaks with weak intensities signify that PACTPPg has little evidence of having an unstructured phase. The peak that resembles TPP could not be recognised probably due to the high concentration of PAC that obscures it in the new reagent.

Similar shifts in the diffraction angles were reported by Azizan [50] when preparing the new composite coagulant of PACTSb made from polyaluminium chloride and commercial tapioca starch (TS) with the optimum concentrations of 90 and 20 g/L for PAC and TS, respectively. According to Azizan [50], the low crystalline properties of TS caused the well-recognised peaks in PACTSb to diffract clearly, similar to the characteristics of PAC. The unstructured phase also occurred due to the relatively weaker peaks of TPP in the deterioration of the ordered structure, which had been remarkably demolished by the graft chain [80]. Meanwhile, a study done

by Yang *et al.* [11] prepared polymeric ferric aluminium sulphate chloride (PFASC) for papermaking wastewater treatment also validated the presence of Al or Fe hydroxide hydrate compounds based on the XRD analysis. Therefore, the XRD results showed that PACTPPg encompassed possible complexion compounds of Al, Fe, Si, Pb, Cl, and other ions in the inorganic-organic interpenetration networks, rather than a simple mixture of raw materials that are reliable to the analyses of FTIR spectroscopy [11, 13, 14].

This finding is also in agreement with the study conducted by Li *et al.* [14] that analysed the XRD spectra of PFM-PDMDAAC, a novel inorganic-organic composite coagulant made from poly-ferric-magnesium (PFM), polydimethyldiallylammonium chloride (PDMDAAC), FeSO4, and MgSO4 as the raw materials. The formation of a new substance with better coagulation properties occurred when the reactions took place between all the respective reagents [14]. In general, the characterisation of PACTPPg through every analysis mentioned above, has answered the early curiosity behind its effectiveness. The intersection point of all respective characteristics of PACTPPg becomes the reason for the composite coagulant to be determined as the optimum weight ratio for the wastewater treatment of the leachate sample.

4. Conclusions

The different weight to weight ratio of different materials gives an essential effect in the development of a new coagulant so that it can work at its best for better coagulation performance. This study was conducted to determine the physicochemical, morphological, and structural properties of new composite coagulant of PACTPP made from polyaluminium chloride (PAC) and agro-waste of Tapioca Peel Powder (TPP). In the preliminary study, the optimum TPP/Al=3.71 weight ratio of PACTPPg was determined as the optimum composite coagulant. Indeed, the new-developed composite coagulant was characterised with low +ζ potential, higher molecular weight, low conductivity, and acidic. Here, even though PACTPPg had lower ζ potential, the increment of its molecular weight made it able to create better coagulation ability. Next, through the analysis of SEM-EDX, it revealed that the morphology of PACTPPg had longer-connected structure; meanwhile, FTIR and XRD analyses prove that the development of PACTPPg consisted of the formation of new compounds alongside improved coagulation properties that occurred when the reactions took place between all the respective reagents. PACTPPg carried the functional groups of hydroxyl, hydrogen bonding, carboxyl, amino or amid groups that favoured it as the effective coagulating agents. The new groups of ketones, aldehydes, and alkanes were also discovered. To conclude, the new PACTPPg coagulant was verified to offer the full role-play of each other's advantages by producing an apparent synergistic effect on its characteristics.

Declarations

Availability of data and materials

The data used to support the findings of this study are available from the corresponding author upon request.

Competing interests

The authors declare they have no competing interests.

Funding

Authors' contributions

Writing—original draft preparation, Mohd-Salleh, S. N. A.; Conceptualisation, Shaylinda, M. Z. N. and Othman, N.; methodology, Shaylinda, M. Z. N.; validation, Mohd-Salleh, S. N. A.; formal analysis, Mohd-Salleh, S. N. A.; investigation, Mohd-Salleh, S. N. A.; data curation, Mohd-Salleh, S. N. A.; writing—review and editing, Yashni, G., Norshila, A. B., and Sainudin, M. S.; supervision, Shaylinda, M. Z. N. and Othman, N. All authors read and approved the final manuscript.

Acknowledgements

References

1. Hesami, F. Bina, B., Ebrahimi, A., & (2014). The effectiveness of chitosan as coagulant aid in turbidity removal from water. *International Journal of Environmental Health Engineering*, 3(1), 8. http://doi.org/10.4103/2277-9183.131814

2. Shaylinda, M. Z. N., Aziz, H. A., Adlan, M. N., Ariffin, A., Yusoff, M. S., & Dahlan, I. (2014). Treatability Study of Partially Stabilized Leachate by Composite Coagulant (Prehydrolyzed Iron and Tapioca Flour). *International Journal of Scientific Research in Knowledge*, (July 2014), 313–319. http://doi.org/10.12983/ijsrk-2014-p0313-0319

3. Kumar, V., Othman, N., & Asharuddin, S.M. (2017). Applications of Natural Coagulants to Treat Wastewater – A Review. *MATEC Web of Conferences,* 103(April), 06016. http://doi.org/10.1051/matecconf/201710306016

4. Syafalni, Lim, H. K., Ismail, N., Abustan, I., Murshed, M. F., & Ahmad, A. (2012). Treatment of landfill leachate by using lateritic soil as a natural coagulant. *Journal of Environmental Management,* 112, 353–359. http://doi.org/10.1016/j.jenvman.2012.08.001

5. Lee, K. E., Morad, N., Teng, T. T., & Poh, B. T. (2012). Development, characterization and the application of hybrid materials in coagulation/flocculation of wastewater: A review. *Chemical Engineering Journal*, 203, 370–386. http://doi.org/10.1016/j.cej.2012.06.109

6. Tzoupanos, N. D., & Zouboulis, A. I. (2011). Preparation, characterisation and application of novel composite coagulants for surface water treatment. *Water Research*, 45(12), 3614–3626. http://doi.org/10.1016/j.watres.2011.04.009

7. Nanko, M. (2009). Definitions and Categories of Hybrid Materials. *The AZo Journal of Materials Online,* (1), 1–12.

8. Moussas, P. A., & Zouboulis, A. I. (2009). A new inorganic-organic composite coagulant, consisting of Polyferric Sulphate (PFS) and Polyacrylamide (PAA). *Water Research,* 43(14), 3511–3524. http://doi.org/10.1016/j.watres.2009.05.015

9. Huang, X., Gao, B., Wang, Y., Yue, Q., Li, Q., & Zhang, Y. (2014). Coagulation performance and flocs properties of a new composite coagulant: Polytitanium-silicate-sulfate. *Chemical Engineering Journal,* 245, 173–179. http://doi.org/10.1016/j.cej.2014.02.018

10. Wang, B., Shui, Y., Liu, P., & He, M. (2017). Preparation, characterization and flocculation performance of the inorganic–organic composite coagulant polyferric chloride and polydimethyldiallylammonium chloride. *Journal of Chemical Technology and Biotechnology*, 92(4), 884–892. http://doi.org/10.1002/jctb.5073

11. Yang, S., Li, W., Zhang, H., Wen, Y., & Ni, Y. (2019). Treatment of paper mill wastewater using a composite inorganic coagulant prepared from steel mill waste pickling liquor. *Separation and Purification Technology*, 209(April 2018), 238–245. http://doi.org/10.1016/j.seppur.2018.07.049

12. Wang, B., Shui, Y., Liu, P., & He, M. (2016). Preparation, characterization and flocculation performance of an inorganic-organic composite coagulant by polyferric chloride and polydimethyldiallylammonium chloride. *Journal of Chemical Technology & Biotechnology,* 92(4), 884–892.

13. Chen, W., Zheng, H., Guo, J., Li, F., Tang, X., Liu, B., & Zhou, Y. (2016). Preparation and Characterization of a Composite Coagulant: Polyferric Titanium Sulfate. *Water, Air, and Soil Pollution,* 227(3), 1–17. http://doi.org/10.1007/s11270-016-2766-6

14. Li, S., Lv, Y., & Liu, Z. (2015). Preparation of composite coagulant of PFM-PDMDAAC and its coagulation performance in treatment of landfill leachate. *Journal of Water Reuse and Desalination,* 5(2), 177. http://doi.org/10.2166/wrd.2015.093

15. Chen, W., Zheng, H., Zhai, J., Wang, Y., Xue, W., Tang, X., Sun, Y. (2014). Characterization and coagulation–flocculation performance of a composite coagulant: poly-ferric-aluminum-silicate-sulfate. *Desalination and Water Treatment*, 56(7), 1–11. http://doi.org/10.1080/19443994.2014.958109

16. Ang, T. H., Kiatkittipong, K., Kiatkittipong, W., Chua, S. C., Lim, J, W., Show, P. L., Bashir, M. J. K., & Ho, Y. C. (2020). Insight on Extraction and Characterisation of Biopolymers as the Green Coagulants for Microalgae Harvesting. *Water,* 12 (1388); 1-31. http://doi:10.3390/w12051388

17. Zhou, L., Zhou, H., & Yang, X. (2019). Preparation and performance of a novel starch-based inorganic / organic composite coagulant for textile wastewater treatment. *Separation and Purification Technology*, 210 (August 2018), 93–99. http://doi.org/10.1016/j.seppur.2018.07.089

18. Sillanpaa, M., Ncibi, M. C., Matilainen, A., & Vepsalainen, M. (2018). Removal of natural organic matter in drinking water treatment by coagulation : A comprehensive review. *Chemosphere,* 190, 54–71. http://doi.org/10.1016/j.chemosphere.2017.09.113

19. Choy, S. Y., Prasad, K. M. N., Wu, T. Y., Raghunandan, M. E., & Ramanan, R. N. (2014). Utilization of plant-based natural coagulants as future alternatives towards sustainable water clarification. *Journal of Environmental Sciences* (China), 26(11), 2178–2189. http://doi.org/10.1016/j.jes.2014.09.024

20. Ghafari, S., Aziz, H. A., & Bashir, M. J. K. (2010). The use of poly-aluminum chloride and alum for the treatment of partially stabilized leachate: A comparative study. *Desalination*, 257(1–3), 110–116. http://doi.org/10.1016/j.desal.2010.02.037

21. Ni, F., Peng, X., He, J., Yu, L., Zhao, J., & Luan, Z. (2012). Preparation and characterization of composite bioflocculants in comparison with dual-coagulants for the treatment of kaolin suspension. *Chemical Engineering Journal,* 213, 195–202. http://doi.org/10.1016/j.cej.2012.10.006

22. Shen, Y. H., & Dempsey, B. A. (1998). Synthesis and speciation of polyaluminum chloride for water treatment. *Environment International,* 24(8), 899–910. http://doi.org/10.1016/ S0160-4120(98)00073-7

23. Zainol, N. A., Aziz, H. A., Yusoff, M. S., & Umar, M. (2011). The use of Polyaluminum Chloride for the treatment of Landfill Leachate via Coagulation and Flocculation processes. *Research Journal of Chemical Sciences,* 1(3), 34–39.

24. Rasool, M. A., Tavakoli, B., Chaibakhsh, N., Pendashteh, A. R., & Mirroshandel, A. S. (2016). Use of a plant-based coagulant in coagulation-ozonation combined treatment of leachate from a waste dumping site. *Ecological Engineering*, 90, 431–437. http://doi.org/10.1016/j.ecoleng.2016.01.057

25. Shaylinda, M. Z. N. (2015). *Treatment of partially stabilized landfill leachate using composite coagulant derived from prehydrolyzed iron and tapioca starch.*D Thesis. Universiti Sains Malaysia.

26. Rui, L. M., Daud, Z., Aziz, A., & Latif, A. (2012). Advanced Science Information Technology Treatment of Leachate by Coagulation-Flocculation using different Coagulants and Polymer: A Review. *International Journal on Advance Science Engineering Information Technology,* 2, 1–4. http://doi.org/10.18517/ijaseit.2.2.166

27. Oladoja, N. A. (2016). Advances in the quest for substitute for synthetic organic polyelectrolytes as coagulant aid in water and wastewater treatment operations. *Sustainable Chemistry and Pharmacy*, 3, 47–58. http://doi.org/10.1016/j.scp.2016.04.001

28. Shamsnejati, S., Chaibakhsh, N., Pendashteh, A. R., & Hayeripour, S. (2015). Mucilaginous seed of Ocimum basilicum as a natural coagulant for textile wastewater treatment. *Industrial Crops and Products,* 69, 40–47. http://doi.org/10.1016/j.indcrop.2015.01.045

29. Theodoro, J. D. P., Lenz, G. F., Zara, R. F., & Bergamasco, R. (2013). Coagulants and Natural Polymers : Perspectives for the Treatment of Water. *Plastic and Polymer Technology,* 2(3), 55–62. http://doi.org/10.1016/S0021-9673(01)01294-8

30. Zhang, M., Xie, L., Yin, Z., Khanal, S. K., & Zhou, Q. (2016). Biorefinery approach for cassava-based industrial wastes: Current status and opportunities. Bioresource Technology, 215, 50–62. http://doi.org/10.1016/j.biortech.2016.04.026

31. Daud, Z., Sari, A., Kassim, M., Aripin, A. M., Awang, H., & Hatta, Z. M. (2013a). Chemical Composition and Morphological of Cocoa Pod Husks and Cassava Peels for Pulp and Paper Production. *Australian Journal of Basic and Applied Sciences,* 7(9), 406–411.

32. Simate, G. S., Ndlovu, S., & Seepe, L. (2015). Removal of heavy metals using cassava peel waste biomass in a multi-stage countercurrent batch operation. *Journal of the Southern African Institute of Mining and Metallurgy,* 115(12), 1137–1141. http://doi.org/10.17159/2411-9717/2015/v115n12a1

33. Adetunji, A. R., Isadare, D. A., Akinluwade, K. J., & Adewoye, O. O. (2015). Waste-to-Wealth Applications of Cassava – A Review Study of Industrial and Agricultural Applications. *Advances in Research,* 4(4), 212–229. http://doi.org/10.9734/AIR/2015/15417

34. Simate, G. S., & Ndlovu, S. (2015). The removal of heavy metals in a packed bed column using immobilized cassava peel waste biomass. *Journal of Industrial and Engineering Chemistry*, 21, 635–643. http://doi.org/10.1016/j.jiec.2014.03.031

35. Ratnadewi, A. A. I., Santoso, A. B., Sulistyaningsih, E., & Handayani, W. (2016). Application of Cassava Peel and Waste as Raw Materials for Xylooligosaccharide Production Using Endoxylanase from Bacillus subtilis of Soil Termite Abdomen. *Procedia Chemistry,* 18, 31–38. http://doi.org/10.1016/j.proche.2016.01.007

36. Candrawati, I., Martak, F., & Ika Cahyo, Y. (2017). Absorption Activity of Cassava Peel (Manihot utilissima) as Chromium (VI) Metal Biosorbent in Electroplating Waste. *The Journal of Pure and Applied Chemistry Research,* 6(2), 101–110. http://doi.org/10.21776/ub.jpacr.2017.006.02.313

37. Versino, F., López, O. V., & García, M. A. (2015). Sustainable use of cassava (Manihot esculenta) roots as raw material for biocomposites development. *Industrial Crops and Products,* 65(March), 79–89. http://doi.org/10.1016/j.indcrop.2014.11.054

38. Aripin, A. M. (2013). Cassava Peels for Alternative Fibre in Pulp and Paper Industry: Chemical Properties and Morphology Characterization. *International Journal of Integrated,* 5(1), 30–33.

39. Jain, M. S., Daga, M., and Kalamdhad, A. S. (2019) Variation in the key indicators during composting of municipal solid organic wastes. *Sustainable Environment Research,* 29:9. 1-8. https://doi.org/10.1186/s42834-019-0012-9

40. Ki, O. L., Kurniawan, A., Lin, C. X., Ju, Y. H., & Ismadji, S. (2013). Bio-oil from cassava peel: A potential renewable energy source. *Bioresource Technology*, 145, 157–161. http://doi.org/10.1016/j.biortech.2013.01.122

41. Edhirej, A., Sapuan, S. M., Jawaid, M., & Zahari, N. I. (2016). Preparation and Characterization of Cassava Starch/Peel Composite Film. *Polymer Composites,* 1-12. http://doi.org/10.1002/pc

42. Yusoff, M. S., Aziz, H. A., Faiz, M. Ah. Z. M., Suja, F., Zuhairi, A. A., & Ezlin, A. B. N. (2018). Floc behavior and removal mechanisms of cross-linked Durio zibethinus seed starch as a natural flocculant for landfill leachate coagulation- flocculation treatment. *Waste Management,* 74, 362–372. http://doi.org/10.1016/j.wasman.2018.01.016

43. Pondja Jr., E. A., Persson, K. M., & Matsinhe, N. P. (2017b). The Potential Use of Cassava Peel for Treatment of Mine Water in Mozambique. *Journal of Environmental Protection,* 08(03), 277–289. http://doi.org/10.4236/jep.2017.83021

44. Asharuddin, S. M., Othman, N., Shaylinda, M. Z. N., & Tajarudin, H. A. (2017). A Chemical and Morphological Study of Cassava Peel: A Potential Waste as Coagulant Aid. *MATEC Web of Conferences,* 103(April), 06012. http://doi.org/10.1051/matecconf/201710306012

45. Salahudeen, N., Ajinomoh, C. S., & Nakakana, S. (2015). Adsorption Isotherm Study for Activated Carbon Produced from Cassava Peel. *Journal of Materials and Metallurgical Engineering,* 4(3), 8–12.

46. Gin, W.A., Jimoh, A., Abdulkareem, A.S. and Giwa, A. (2014). Utilization of Cassava Peel Waste as a Raw Material for Activated Carbon Production: Approach to Environmental Protection in Nigeria. *International Journal of Engineering Research and Technology,* 3(1), 35–42.

47. Zayadi, N., Othman, N., & Hamdan, R. (2016). A Potential Waste to be Selected as Media for Metal and Nutrient Removal. *IOP Conference Series: Materials Science and Engineering,* 136(1). http://doi.org/10.1088/1757-899X/136/1/012051

48. Harfouchi, H., Hank, D., & Hellal, A. (2016). Response surface methodology for the elimination of humic substances from water by coagulation using powdered Saddled sea bream scale as coagulant-aid. *Process Safety and Environmental Protection,* 99, 216–226. http://doi.org/10.1016/j.psep.2015.10.019

49. Fatehah, M. O., Hossain, S., & Teng, T. T. (2013). Semiconductor Wastewater Treatment Using Tapioca Starch as a Natural Coagulant. *Journal of Water Resource and Protection,* 05(11), 1018–1026. http://doi.org/10.4236/jwarp.2013.511107

50. Azizan, M. O. (2019). *Leachate treatment by using composite coagulant made from polyaluminium chloride (PAC) and tapioca starch (TS).* Master Thesis. Universiti Tun Hussien Onn Malaysia.

51. Afanga, H., Zazou, H., Titchou, F. E., Rakhila, Y. (2020) Integrated electrochemical processes for textile industry wastewater treatment: system performances and sludge settling characteristics. *Sustainable Environment Research*, 30:2, 1-11. https://doi.org/10.1186/s42834-019-0043-2

52. American Public Health Association (APHA) (2017). Standard method for examination of water and wastewater, 23rd edn. APHA, AWWA, WPCF, Washington.

53. Lo, M.R. (2012). *Development and Application of Novel Coagulant from Oil Palm Trunk Waste for Semi-Aerobic Landfill Leachate Treatment.* Master Thesis. Universiti Sains Malaysia.

54. Fatombi, J. K., Lartiges, B., Aminou, T., Barres, O., & Caillet, C. (2013). A natural coagulant protein from copra (Cocos nucifera) : Isolation , characterization , and potential for water purification. *Separation and Purification Technology*, 116, 35–40. http://doi.org/10.1016/j.seppur.2013.05.015

55. Kakoi, B., Kaluli, J. W., Ndiba, P., & Thiong'o, G. (2016). Banana pith as a natural coagulant for polluted river water. *Ecological Engineering,* 95, 699–705. http://doi.org/10.1016/j.ecoleng.2016.07.001

56. Maurya, S., & Daverey, A. (2018). Evaluation of plant based natural coagulants for municipal wastewater treatment. *Biotech*, 8(77), 1–4. http://doi.org/10.1007/s13205-018-1103-8.

57. Misau, I. M., & Yusuf, A. A. (2016). Characterization of Water Melon Seed Used As Water Treatment Coagulant. Advanced Studies in Agricultural, *Biological and Environmental Sciences*, 3(2), 22–29.

58. Shak, K. P. Y., & Wu, T. Y. (2014). Coagulation-flocculation treatment of high-strength agro-industrial wastewater using natural Cassia obtusifolia seed gum: Treatment efficiencies and flocs characterization. *Chemical Engineering Journal*, 256, 293–305. http://doi.org/10.1016/j.cej.2014.06.093

59. Oladoja, N. A. (2015). Headway on natural polymeric coagulants in water and wastewater treatment operations. *Journal of Water Process Engineering*, 6, 174–192. http://doi.org/10.1016/j.jwpe.2015.04.004

60. López-Maldonado, E. A., Oropeza-Guzman, M. T., Jurado-Baizaval, J. L., & Ochoa-Terán, A. (2014). Coagulation-flocculation mechanisms in wastewater treatment plants through zeta potential measurements. *Journal of Hazardous Materials*, 279, 1–10. http://doi.org/10.1016/j.jhazmat.2014.06.025

61. Al-Hamadani, Y. A. J., Yusoff, M. S., Umar, M., Bashir, M. J. K., & Adlan, M. N. (2011). Application of psyllium husk as coagulant and coagulant aid in semi-aerobic landfill leachate treatment. *Journal of Hazardous Materials*, 190(1–3), 582–587. http://doi.org/10.1016/j.jhazmat.2011.03.087

62. Rusdizal, N., Aziz, H. A., & Mohd-Omar, F. (2015). Potential use of polyaluminium chloride and tobacco leaf as coagulant and coagulant aid in post-treatment of landfill leachate. *Avicenna J Environmental Health Engineering In Press*, 1–5. http://doi.org/10.1007/978-3-7091-0693-8

63. Ong, S.L. (2010). *A study of landfill leachate treatment by PACl, Sago starch and Tapioca starches, Hymenocallis Liriosme and Aloe Vera as coagulant.* Master Thesis. Universiti Sains Malaysia.

64. Bratby, J. (2006). Coagulation and flocculation in water and wastewater treatment. 2nd Edition, IWA Publishing. Retrieved from iwapublishing.com

65. Amran, A. H., Zaidi, N. S., Muda, K., & Loan, L. W. (2018). Effectiveness of Natural Coagulant in Coagulation Process: A Review. *International Journal of Engineering & Technology*, 7(3.9), 34–37.

66. Emenike, C. U., Fauziah, S. H., & Agamuthu, P. (2012). Characterization and toxicological evaluation of leachate from closed sanitary landfill. *Waste Management & Research*, 30(9), 888–897. http://doi.org/10.1177/0734242X12443585

67. Teh, C. Y., Budiman, P. M., Shak, K. P. Y., & Wu, T. Y. (2016). Recent Advancement of Coagulation-Flocculation and Its Application in Wastewater Treatment. *Industrial and Engineering Chemistry Research*, 55(16), 4363–4389. http://doi.org/10.1021/acs.iecr.5b04703

68. Zouboulis, A., Traskas, G. and Samaras, P. (2008). Comparison of efficiency between polyaluminium chloride and aluminium sulphate coagulants during full-scale experiments in a drinking water treatment plant. *Separation Science Technology*, 43, 1507–1519.

69. Gao, B. Y., Chu, Y. B., Yue, Q. Y., Wang, B. J., & Wang, S. G. (2005). Characterization and coagulation of a polyaluminum chloride (PAC) coagulant with high Al13 content. *Journal of Environmental Management*, 76(2), 143–147. http://doi.org/10.1016/j.jenvman.2004.12.006

70. Tang, H., Xiao, F., & Wang, D. (2015). Speciation, stability, and coagulation mechanisms of hydroxyl aluminum clusters formed by PACl and alum: A critical review. *Advances in Colloid and Interface Science*, 226, 78–85. http://doi.org/10.1016/j.cis.2015.09.002

71. Shi, B., Li, G., Wang, D., & Tang, H. (2007). Separation of Al13 from polyaluminum chloride by sulfate precipitation and nitrate metathesis. *Separation and Purification*, 54(1), 88–95. http://doi.org/10.1016/j.seppur.2006.08.011

72. Tzoupanos, N. D., Zouboulis, A. I., & Tsoleridis, C. A. (2009). A systematic study for the characterization of a novel coagulant (polyaluminium silicate chloride). *Colloids and Surfaces A: Physicochemical and Engineering Aspects*, 342(1-3), 30-39.

73. Choy, S. Y., Prasad, K. N., Wu, T. Y., Raghunandan, M. E., & Ramanan, R. N. (2016). Performance of conventional starches as natural coagulants for turbidity removal. *Ecological Engineering*, 94, 352–364. http://doi.org/10.1016/j.ecoleng.2016.05.082

74. Oladayo, O. O., Umunna, Q. C., Joseph, O. S., & Oluwasegun, W. (2016). Physicochemical properties of cassava starch and starch-keratin prepared biofilm. *Songklanakarin Journal of Science and Technology*, 38(4), 349–355. http://doi.org/10.1016/j.jadohealth.2018.04.003

75. Xu, M., Wu, C., Li, Y., Zhou, Y., Xue, H., & Yu, Y. (2018). Coagulation Behavior and Floc Properties of Dosing Different Alkaline Neutralizers into the Fenton Oxidation Effluent. *Water, Air, & Soil Pollution,* 229(382), 1–12.

76. Niu, X., Li, X., Zhao, J., Ren, Y., & Yang, Y. (2011). Preparation and coagulation efficiency of polyaluminium ferric silicate chloride composite coagulant from wastewater of high-purity graphite production. *Journal of Environmental Sciences,* 23(7), 1122–1128. http://doi.org/10.1016/S1001-0742(10)60537-2

77. Zhu, G., Zheng, H., Chen, W., Fan, W., Zhang, P., & Tshukudu, T. (2012). Preparation of a composite coagulant: Polymeric aluminum ferric sulfate (PAFS) for wastewater treatment. *Desalination*, 285, 315–323. http://doi.org/10.1016/j.desal.2011.10.019

78. Moradi, M., Fazlzadehdavil, M., Pirsaheb, M., & Mansouri, Y. (2016). Response surface methodology (RSM) and its application for optimization of ammonium ions removal from aqueous solutions by pumice as a natural and low cost adsorbent. *Archives of Environmental Protection,* 42(2), 33–43. http://doi.org/10.1515/aep-2016-0018

79. Zouboulis, A. I., Tzoupanos, N. D., and Moussas, P.A. (2007). Inorganic pre-polymerized coagulants:current status and future trends. *In Proceeding of 3rd IASME/WSEAS International Conference on Energy, Environment and Sustainable Development, Agios Nikolaos, Greece.* Retrieved from https://www.researchgate.net/publication/228628710_Inorganic_prepolymerized_coagulants_Current_status_and_future_trends

80. Ma, J., Fu, K., Shi, J., Sun, Y., Zhang, X., & Ding, L. (2016). Ultraviolet-assisted synthesis of polyacrylamide-grafted chitosan nanoparticles and flocculation performance. *Carbohydrate Polymers,* 151, 565–575. http://doi.org/10.1016/j.carbpol.2016.06.002
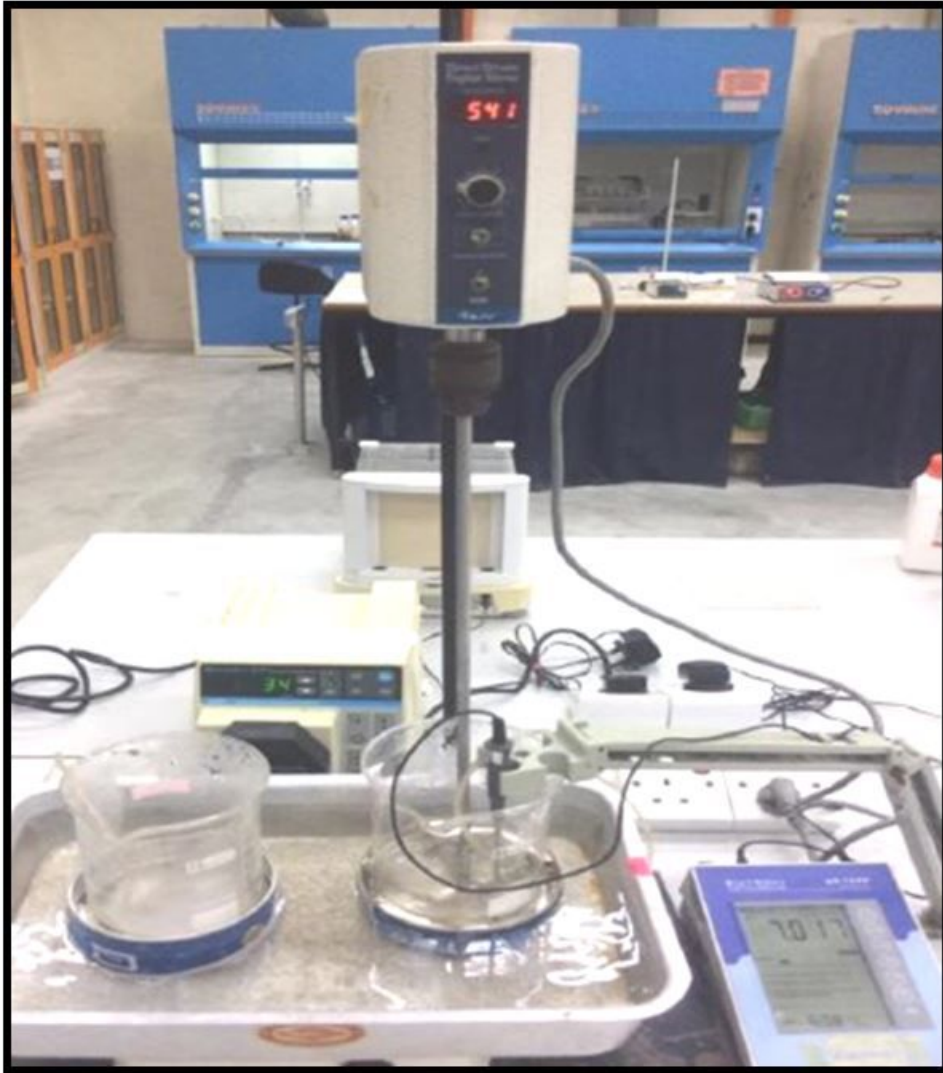
Figures

Figure 1

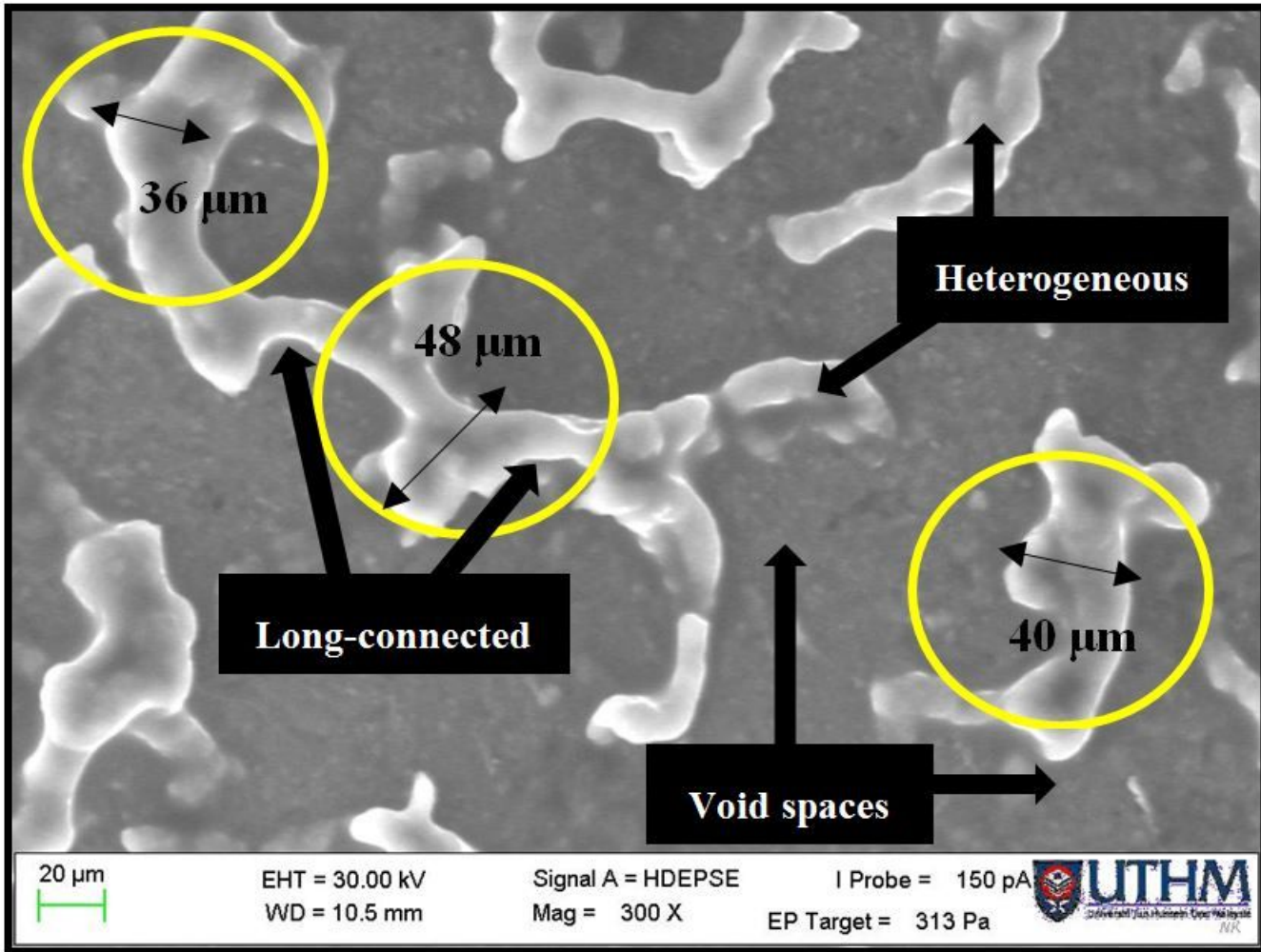The laboratory set-up for the preparation of PACTPP

Figure 2

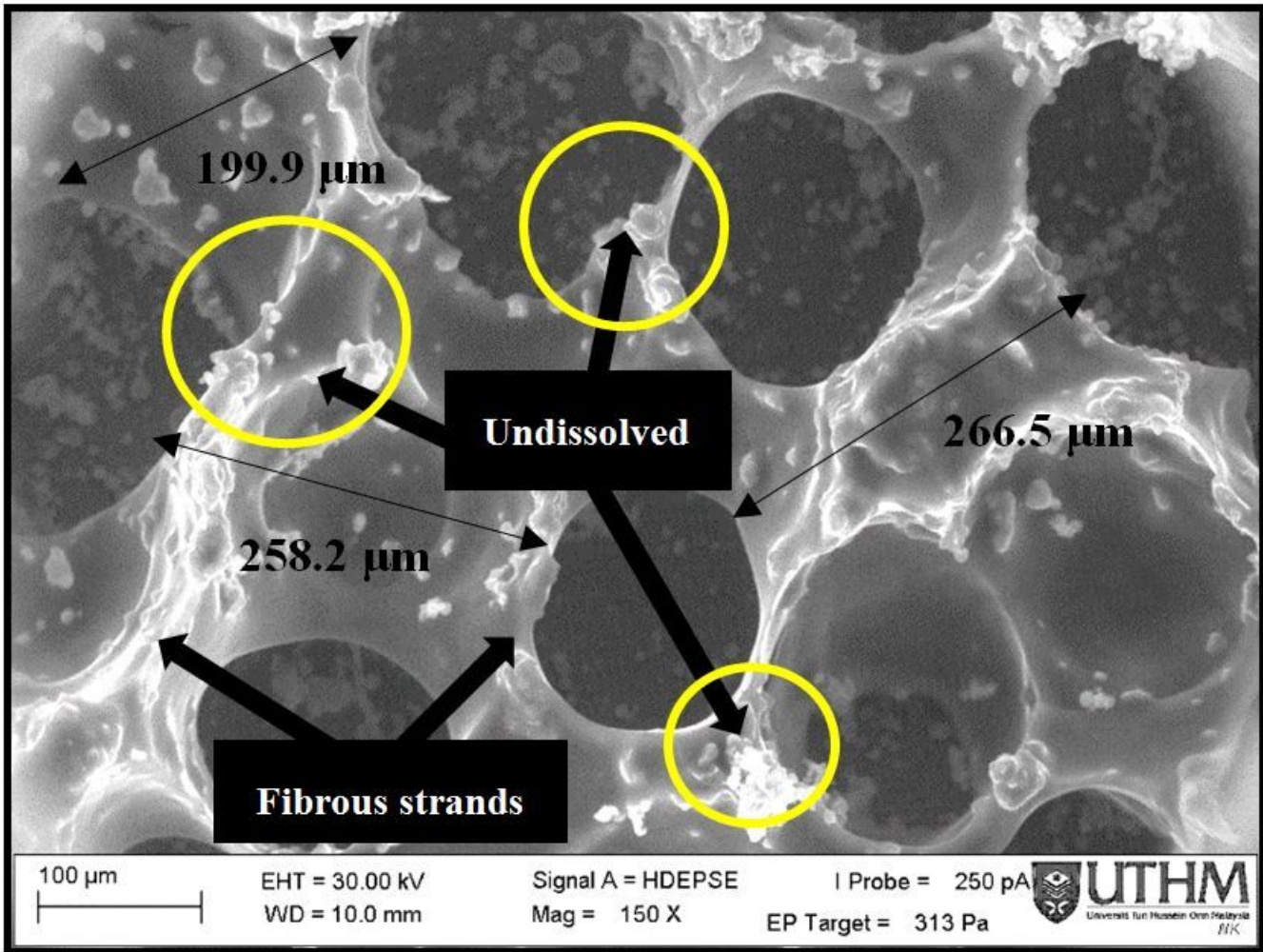SEM image of 10% PAC solution at 300× magnification

Figure 3

SEM image of 1% TPP solution at 150× magnification

Figure 4
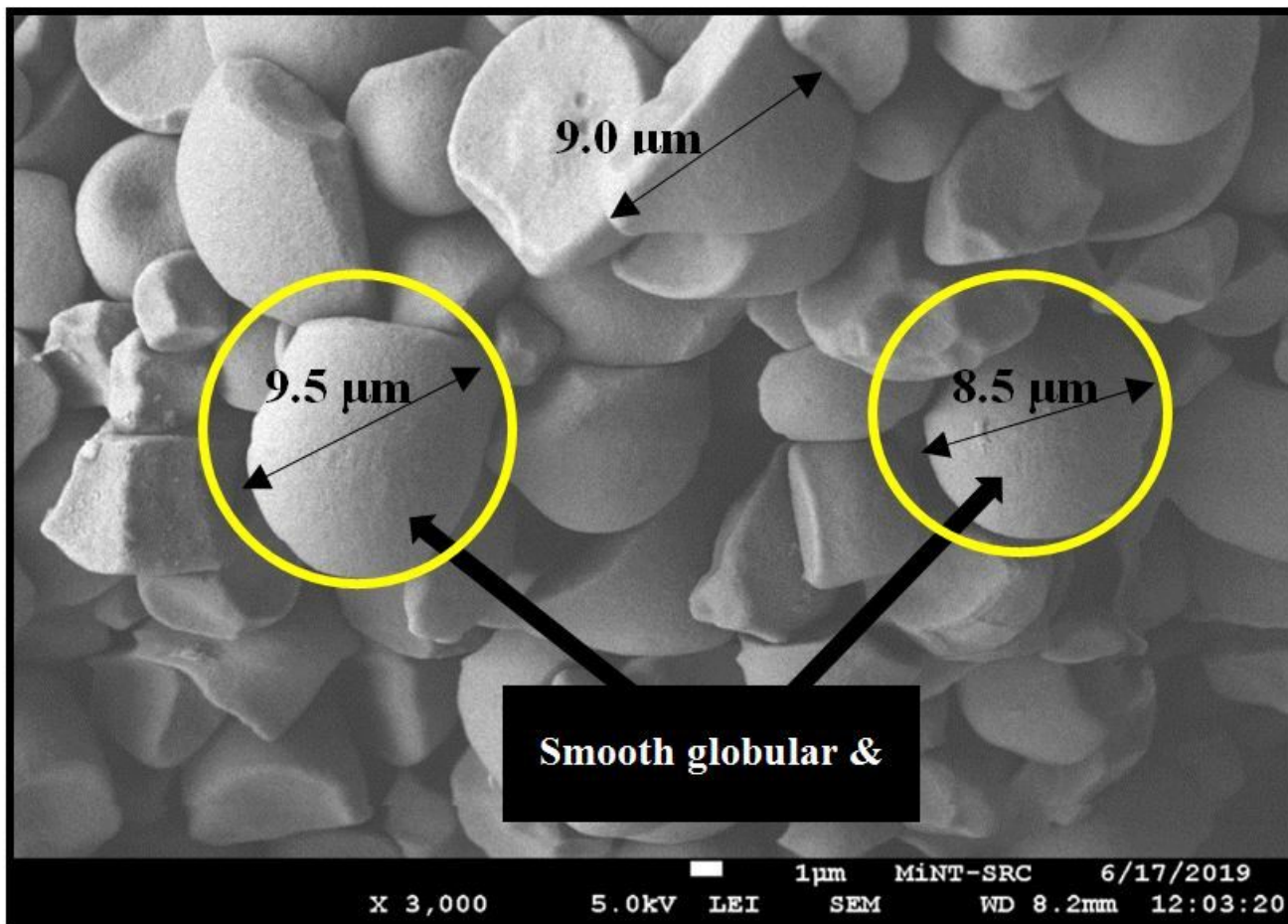
SEM image of raw TPP solution at 3,000× magnification
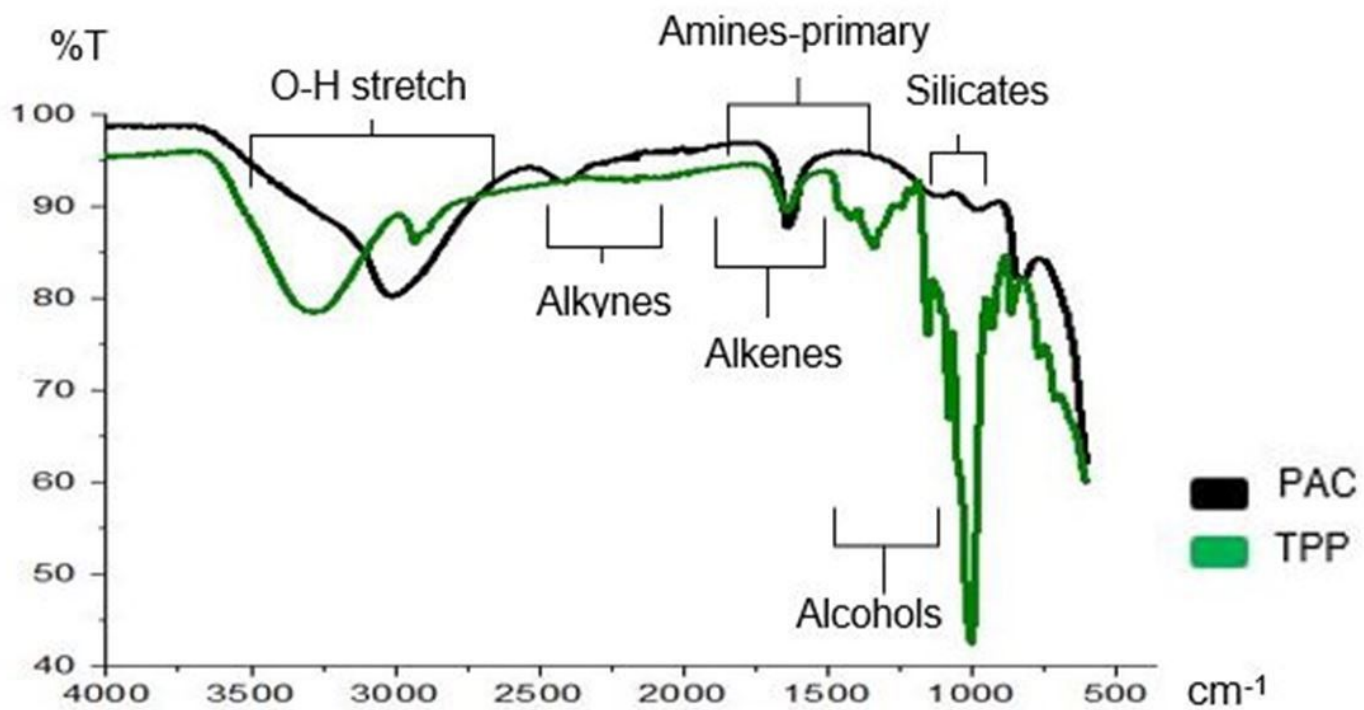
Figure 5
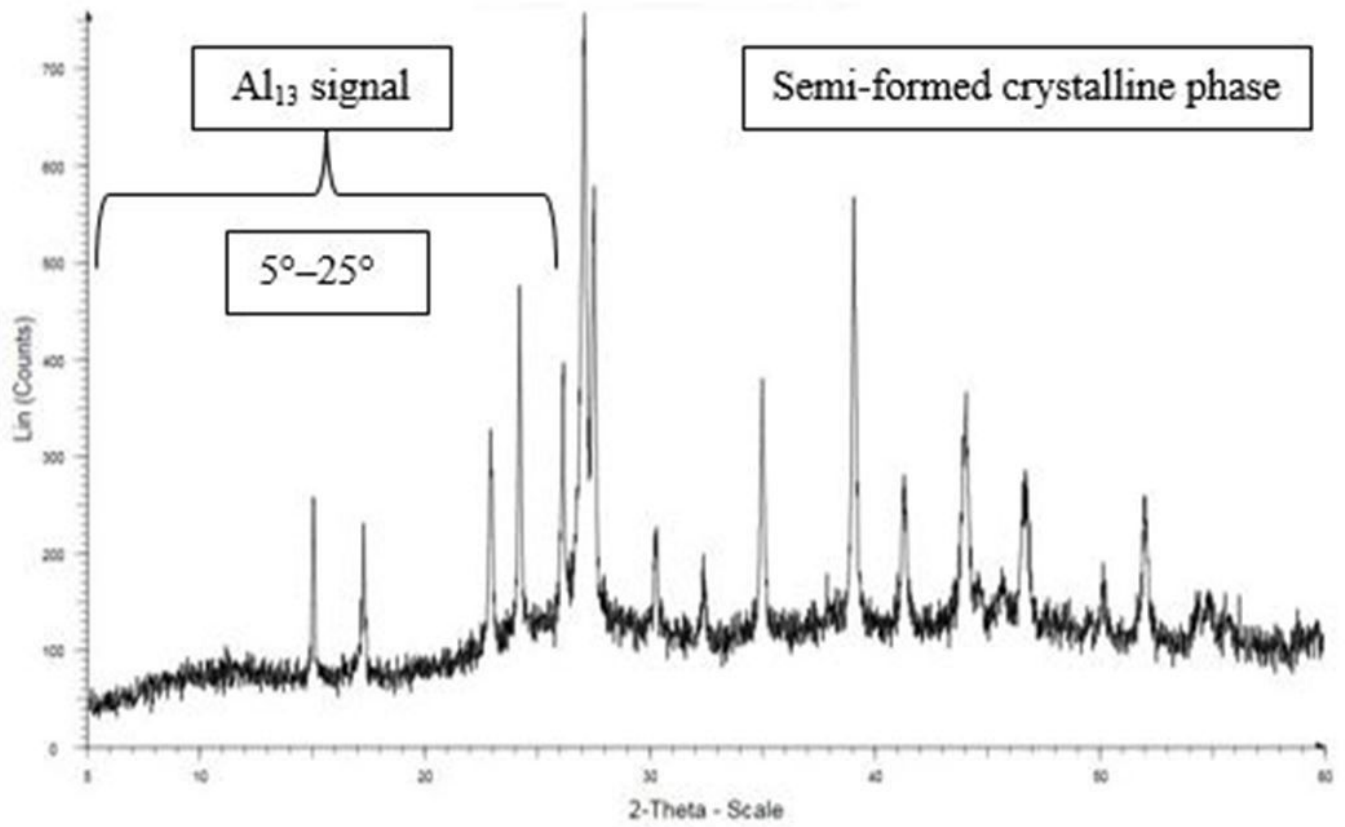
FTIR spectra of raw PAC and TPP coagulants

Figure 6
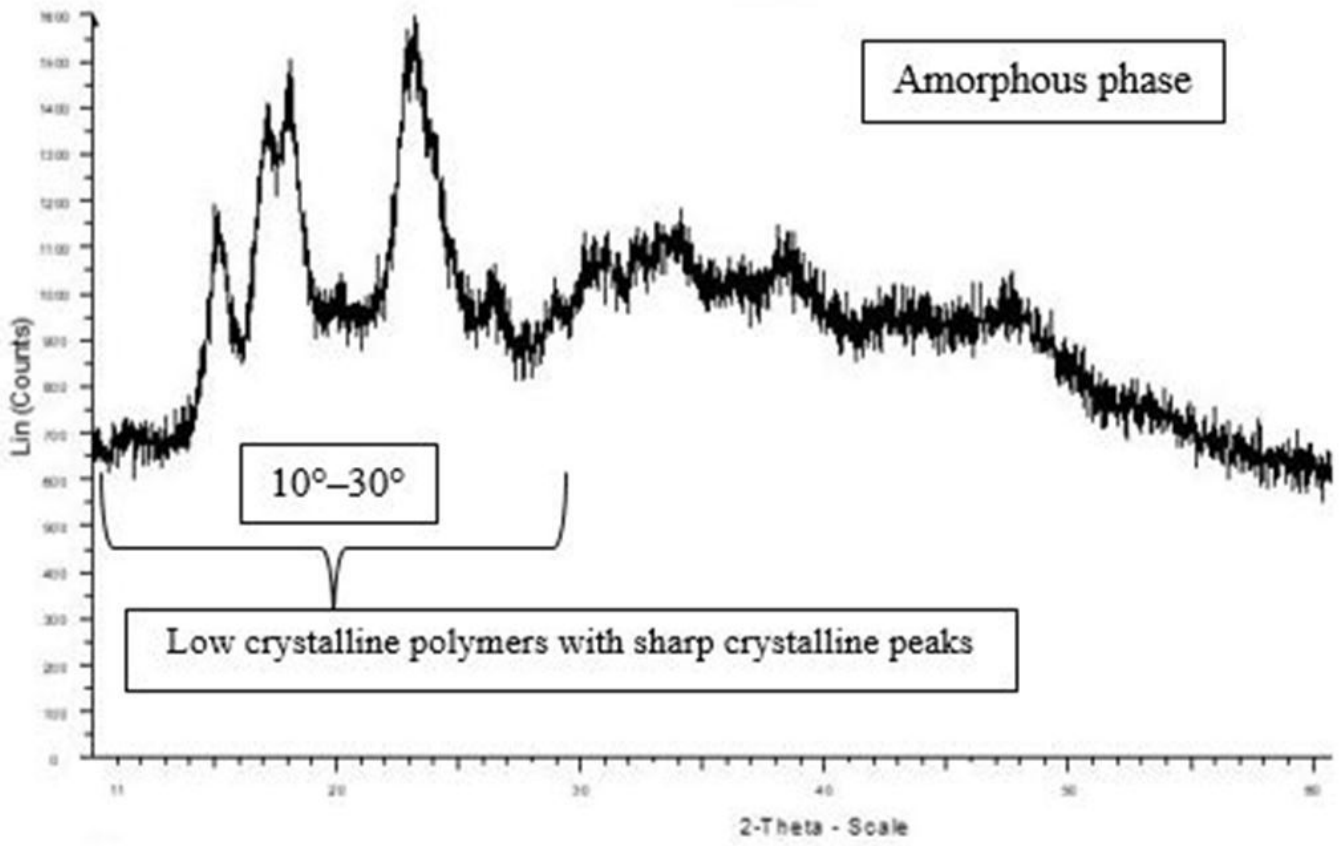
XRD spectra of raw PAC coagulant
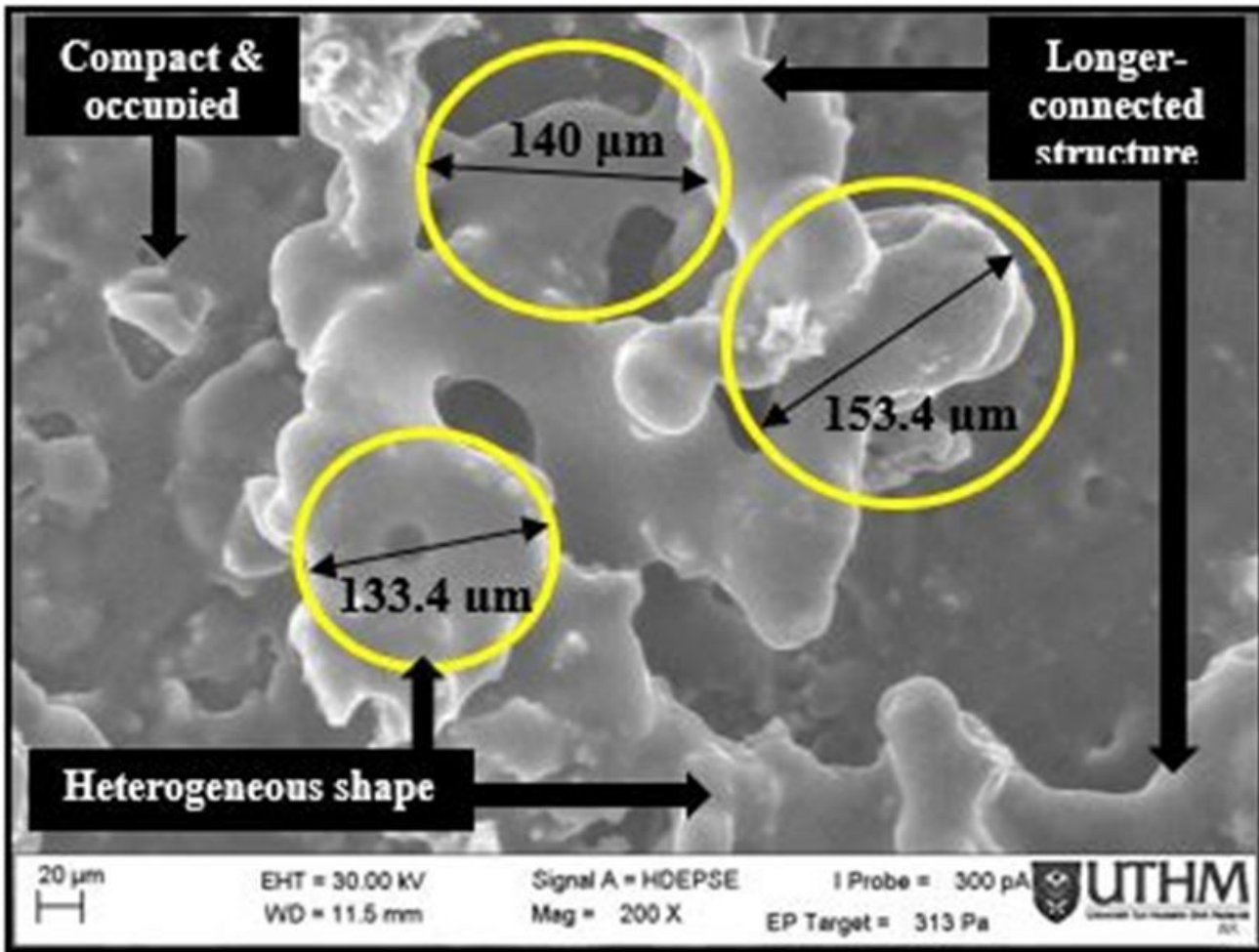
Figure 7

XRD spectra of raw TPP coagulant

Figure 8

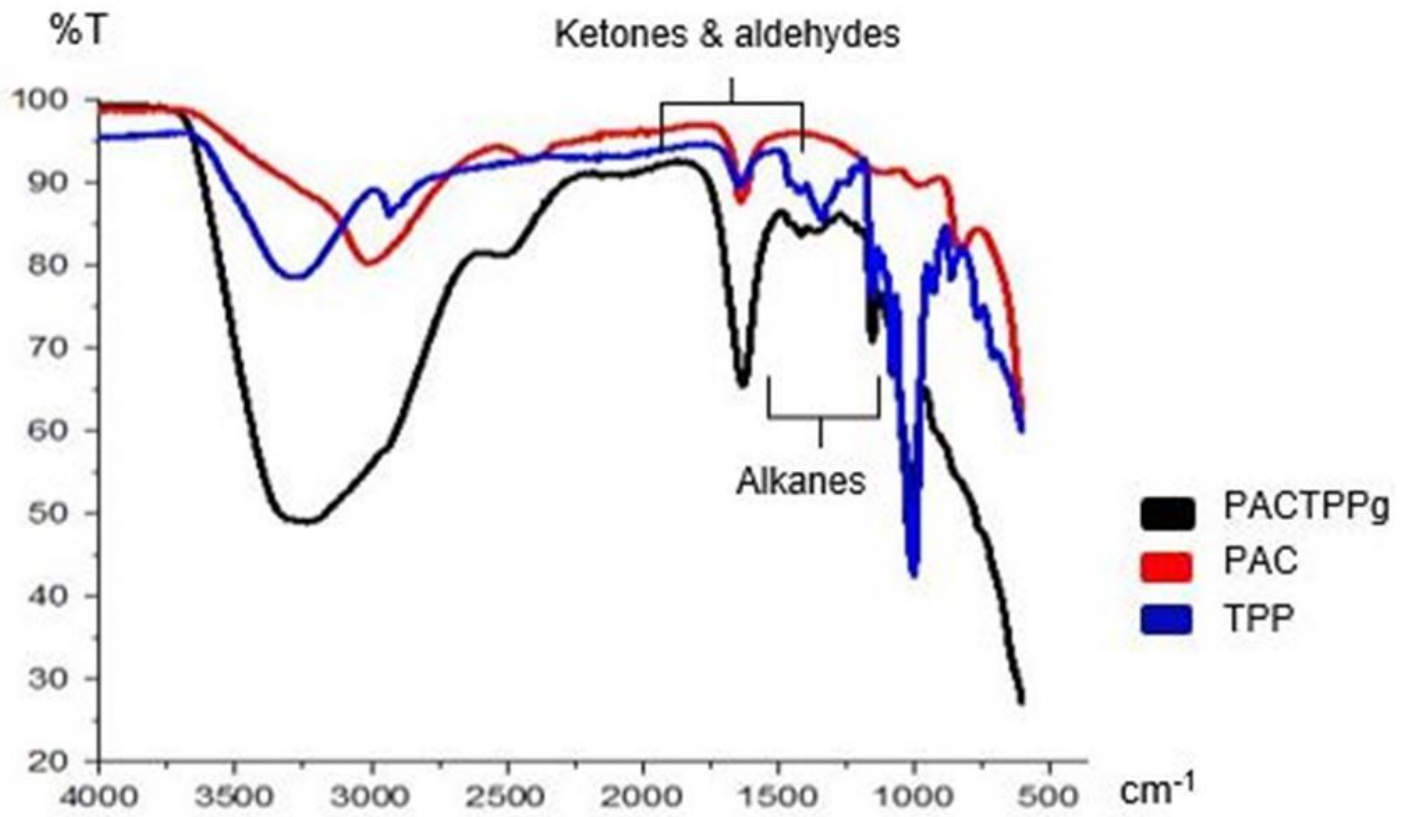SEM image of PACTPPg solution at 200× magnification

Figure 9

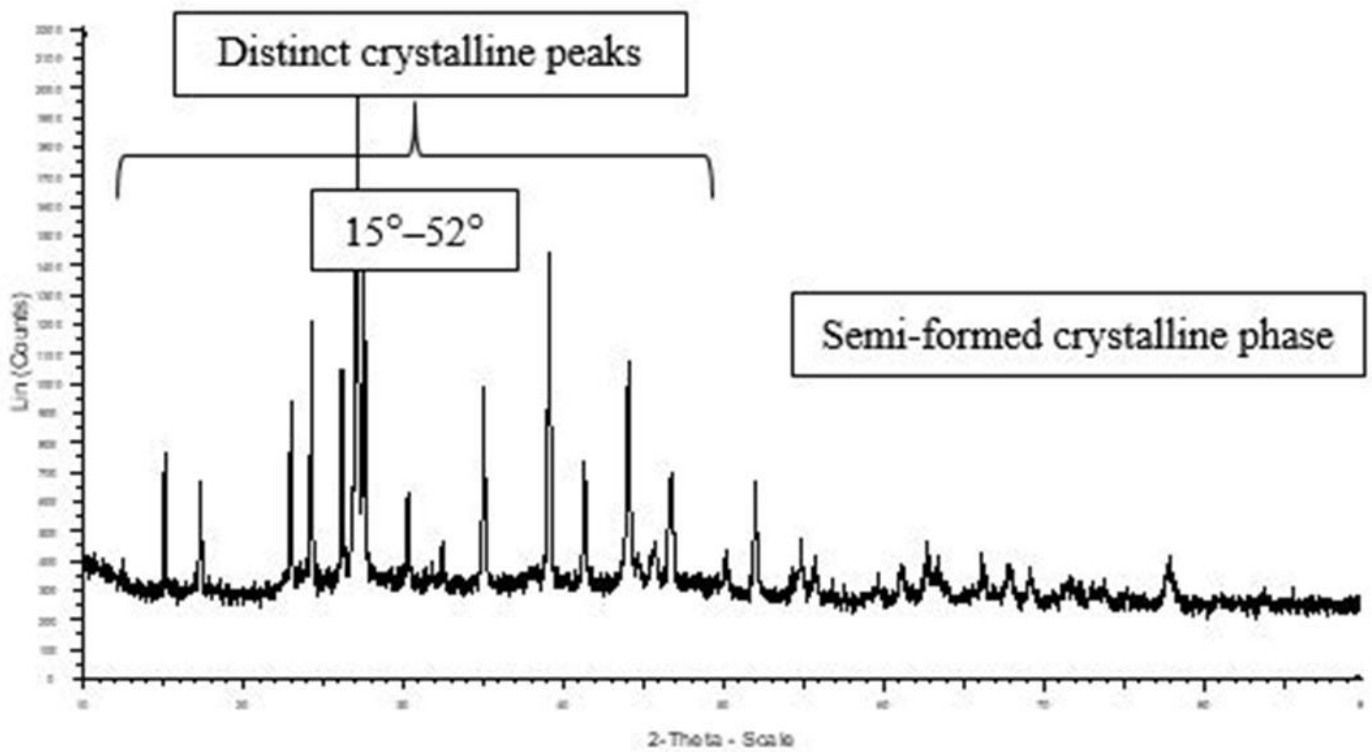FTIR spectra of PACTPPg, PAC, and TPP coagulants

Figure 10

XRD spectra of PACTPPg

Supplementary Files

This is a list of supplementary files associated with this preprint. Click to download.

- AppendixSupplementaryMaterial.docx